

Optical Molecular Imaging

Fluorescence and Bioluminescence Tomography

Alexander D. Klose

Department of Radiology

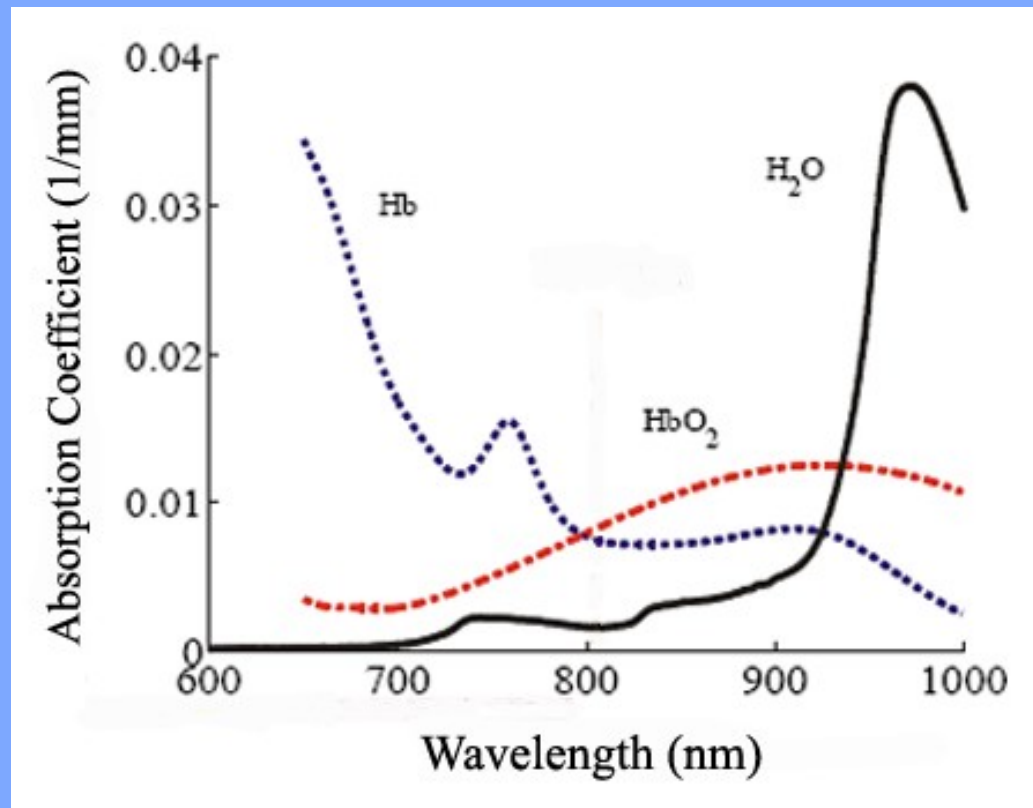
Columbia University

New York





Optical Window Of Biological Tissue



Levels of Optical Imaging

Optical Imaging



imaging of non-specific changes related to morphology and physiology

endogenous chromophores or non-specific contrast agents

developed disease

Optical *Molecular* Imaging



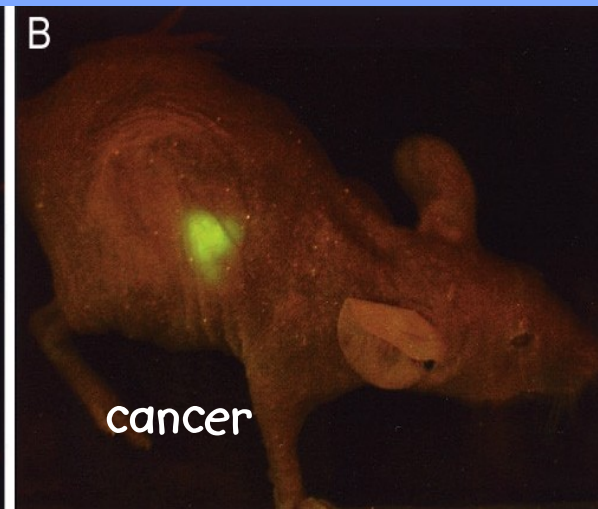
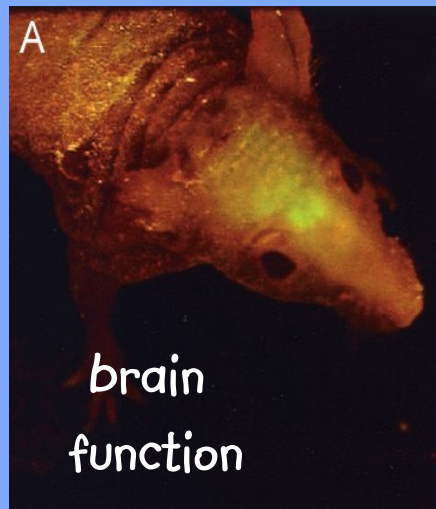
imaging of location and expression levels of specific genes and proteins that are part in the molecular pathways of disease

targeted fluorescent probes

early disease

Optical Molecular Imaging

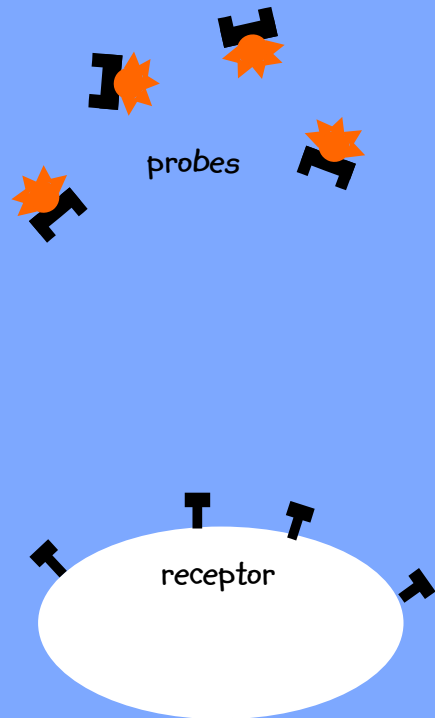
Fluorophore concentration?



fluorescence light on tissue surface

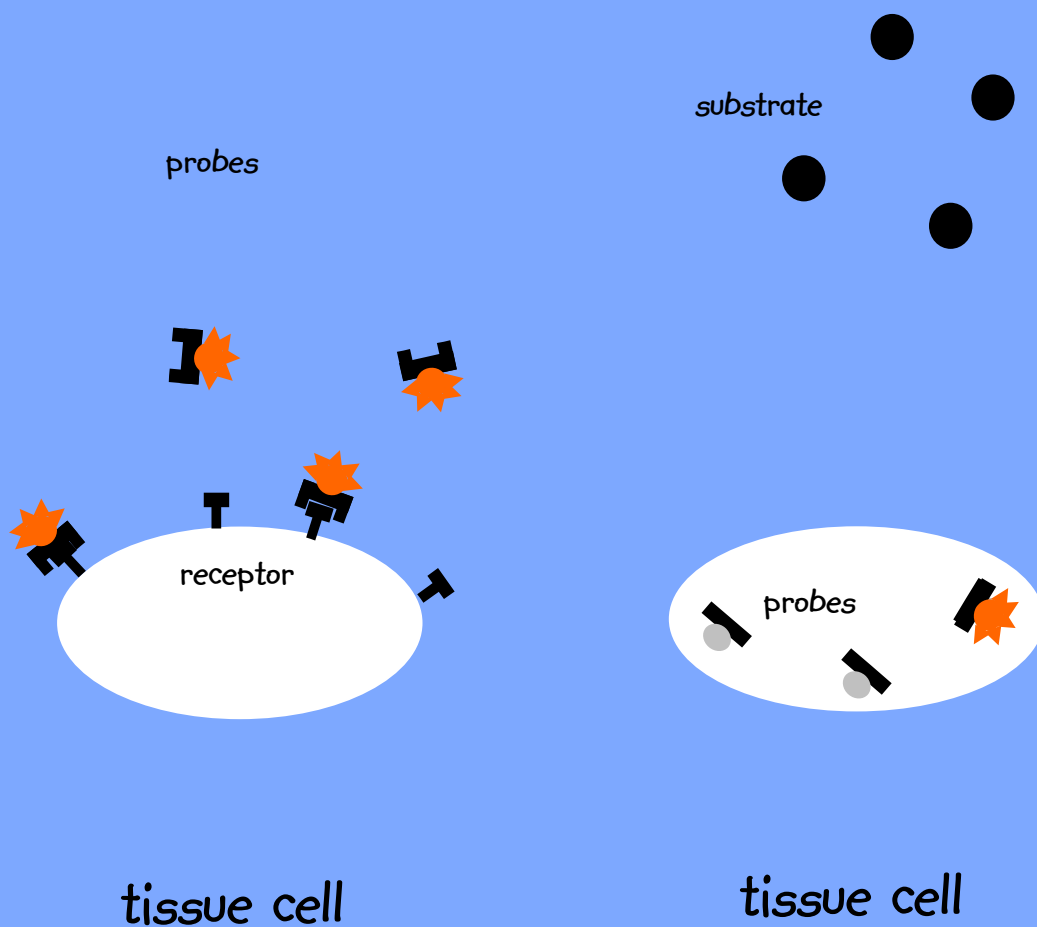


Optical Molecular Imaging



tissue cell

Optical Molecular Imaging



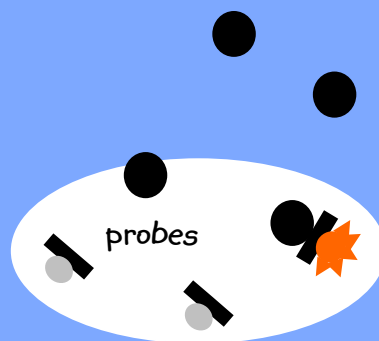


Optical Molecular Imaging

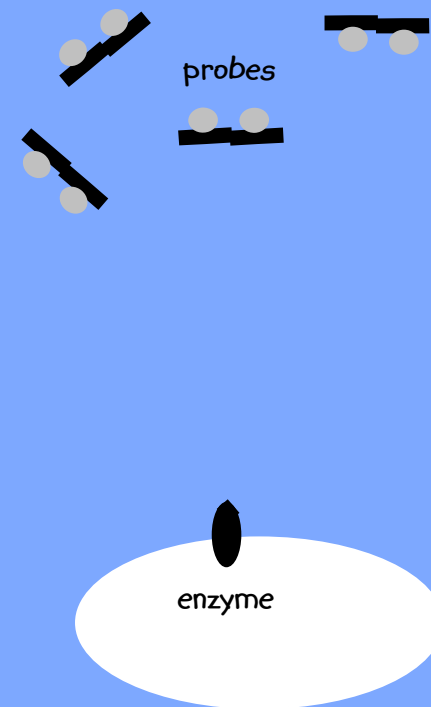


tissue cell

substrate

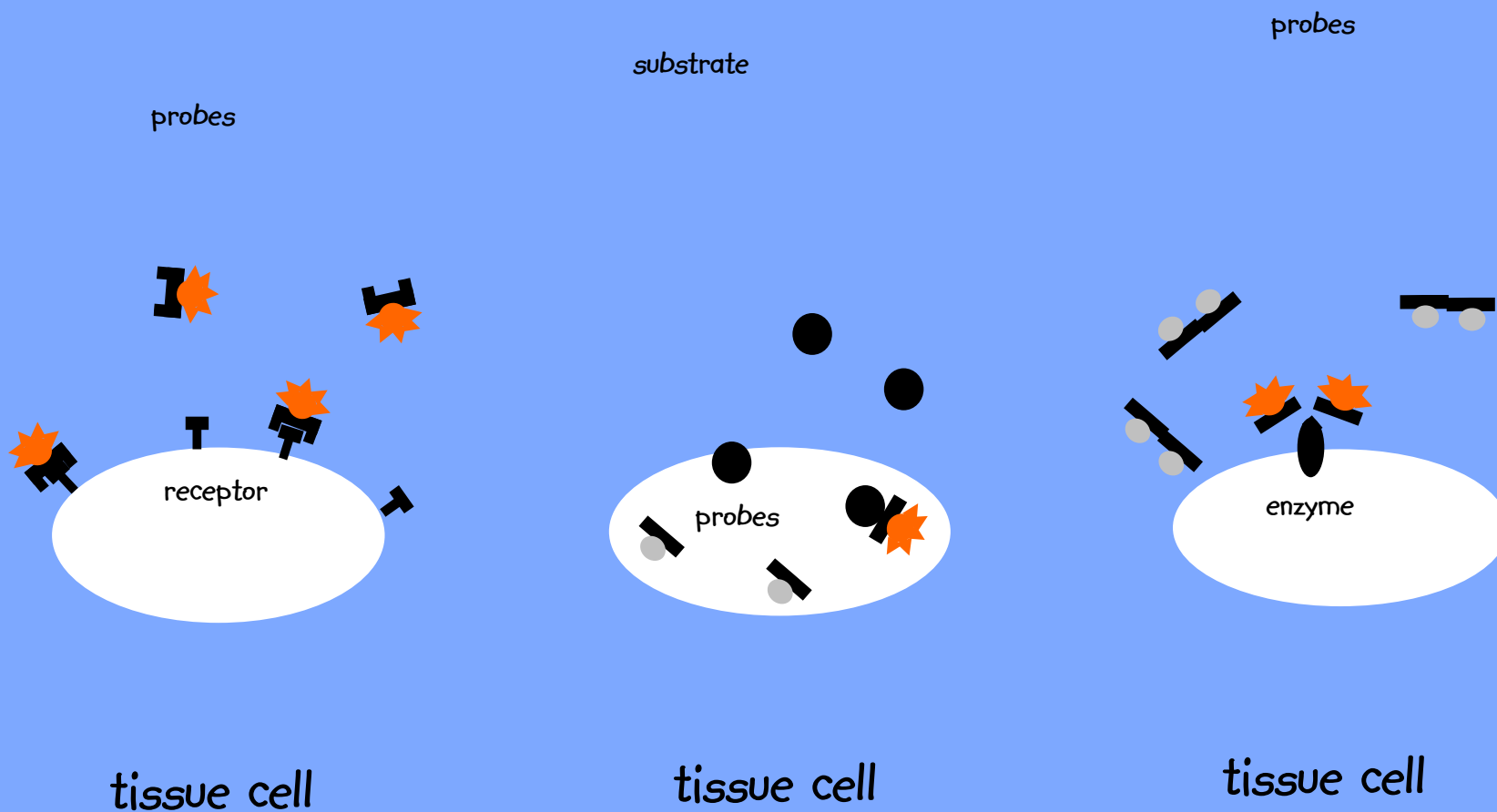


tissue cell



tissue cell

Optical Molecular Imaging

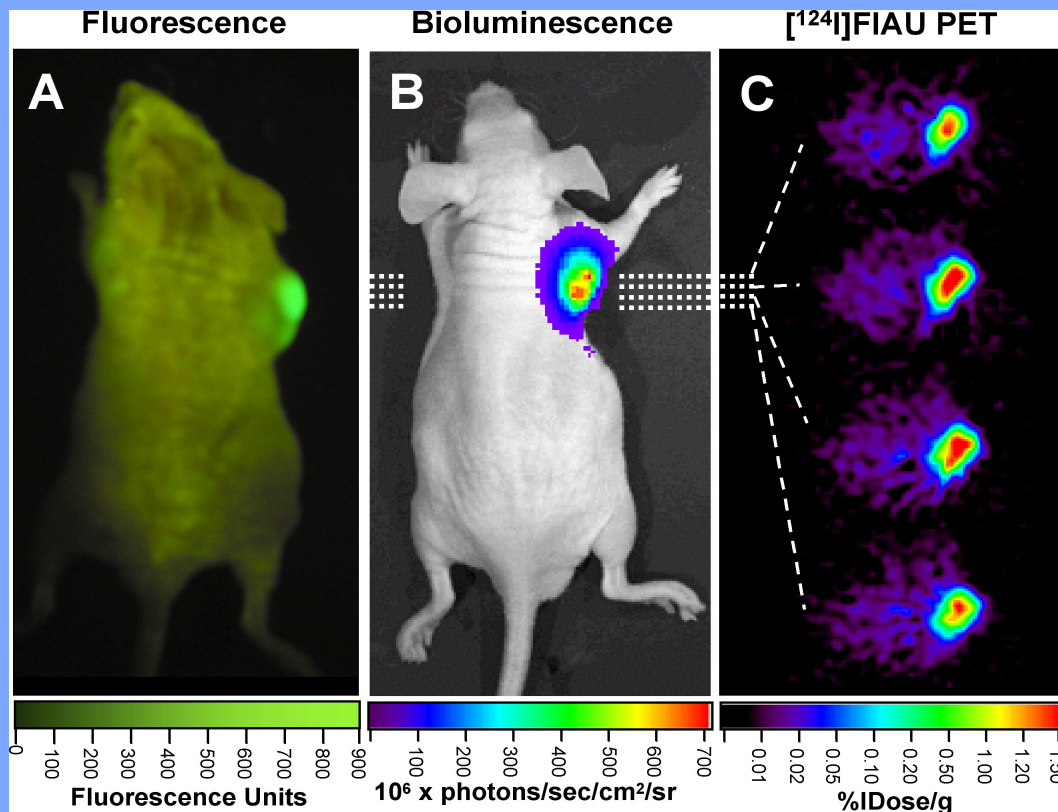




Optical Reporter Probes

Agent	Excitation [nm]	Emission [nm]	Extinction [cm ⁻¹ M ⁻¹]	Quantum Yield
Dye:				
Cy5	649	670	250,000	0.28
Cy5.5	675	694	250,000	0.28
Cy7	743	767	200,000	0.29
Protein:				
GFP	489	508	55,000	0.6
DsRed	558	583	57,000	0.79
Catalyst-Substrate:				
Luciferase/ Luciferin	N.A.	560	N.A.	0.88

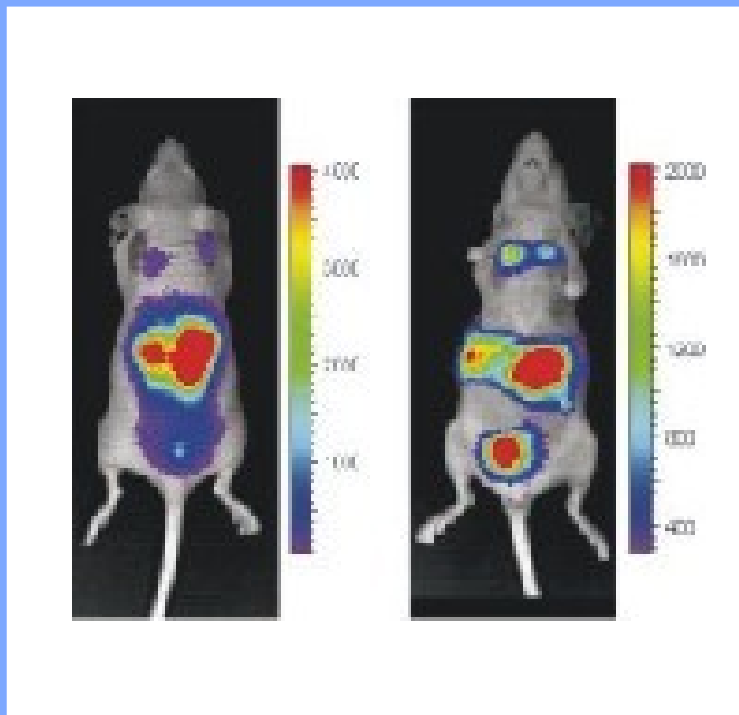
Optical Molecular Tomography?



Mouse bearing two subcutaneous xenografts
(U87-NES-HSV1-tk/GFPcmvFluc - right shoulder)

Inverse Source Problem

measured light intensity



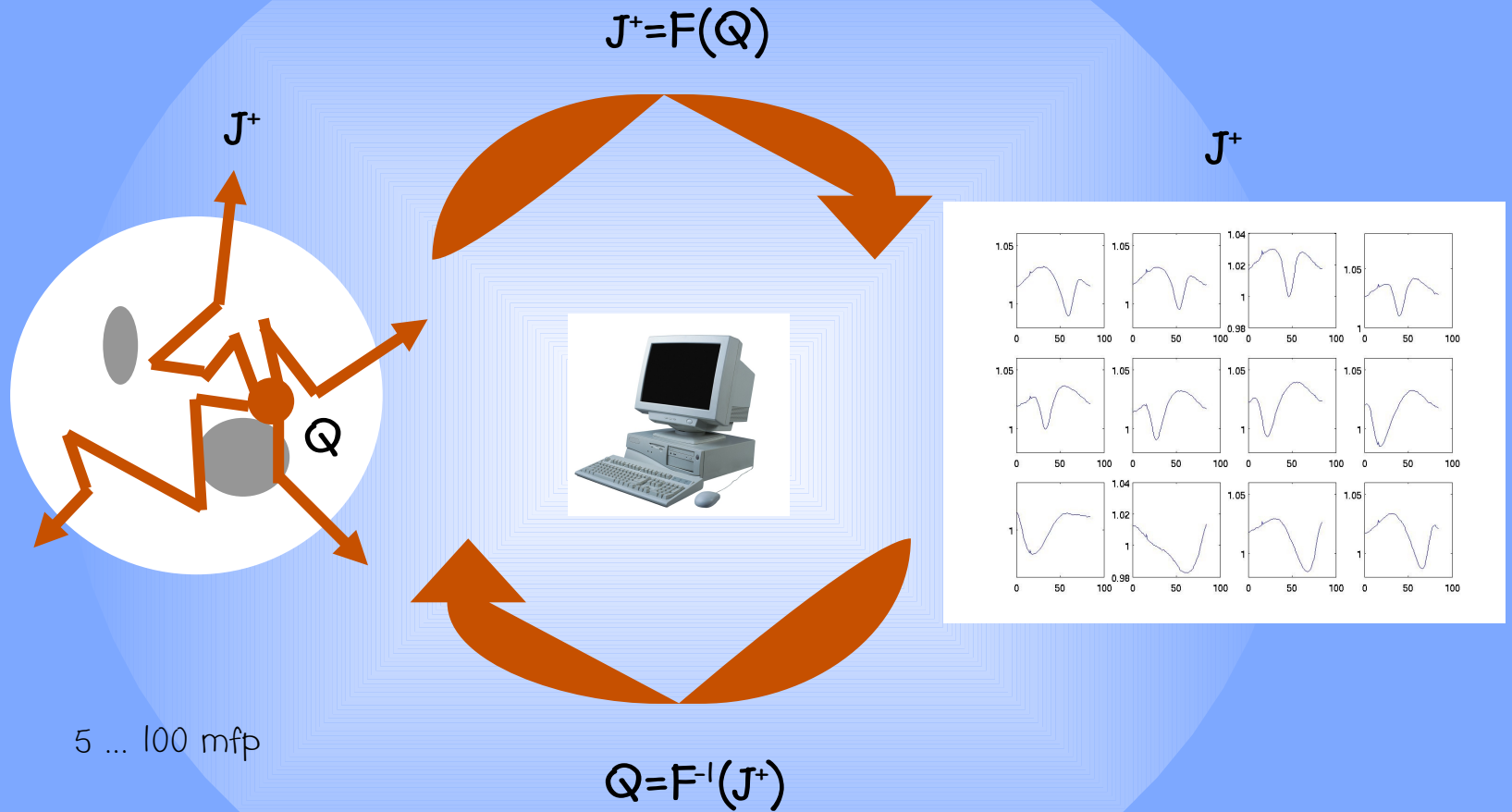
boundary current J^+
[Watts cm^{-2}]
[photons $\text{s}^{-1} \text{cm}^{-2}$]

reconstructed source



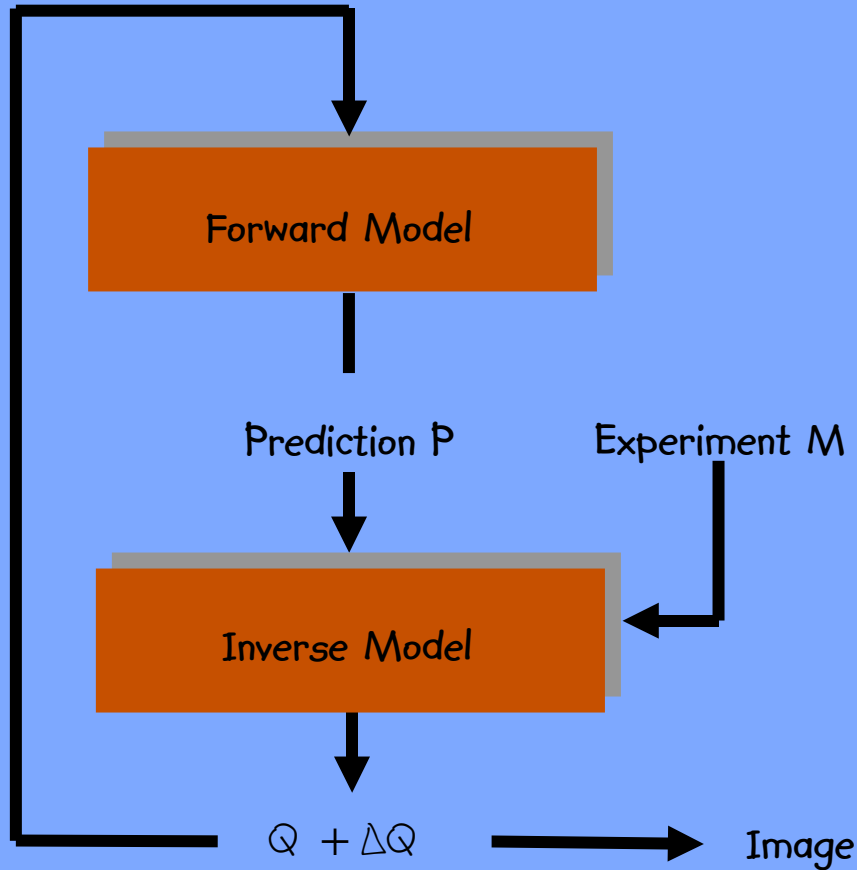
source power density Q
[Watts cm^{-3}]
[photons $\text{s}^{-1} \text{cm}^{-3}$]

Inverse Source Problem





Optimization Problem – Error Function



Error Function:

$$\phi(Q) = \frac{1}{N} \sum_n \frac{(M_n - P_n(Q))^2}{\sigma_n^2}$$



Overview

Forward Model

Inverse Model

Fluorescence Molecular Tomography

Bioluminescence Tomography



Overview

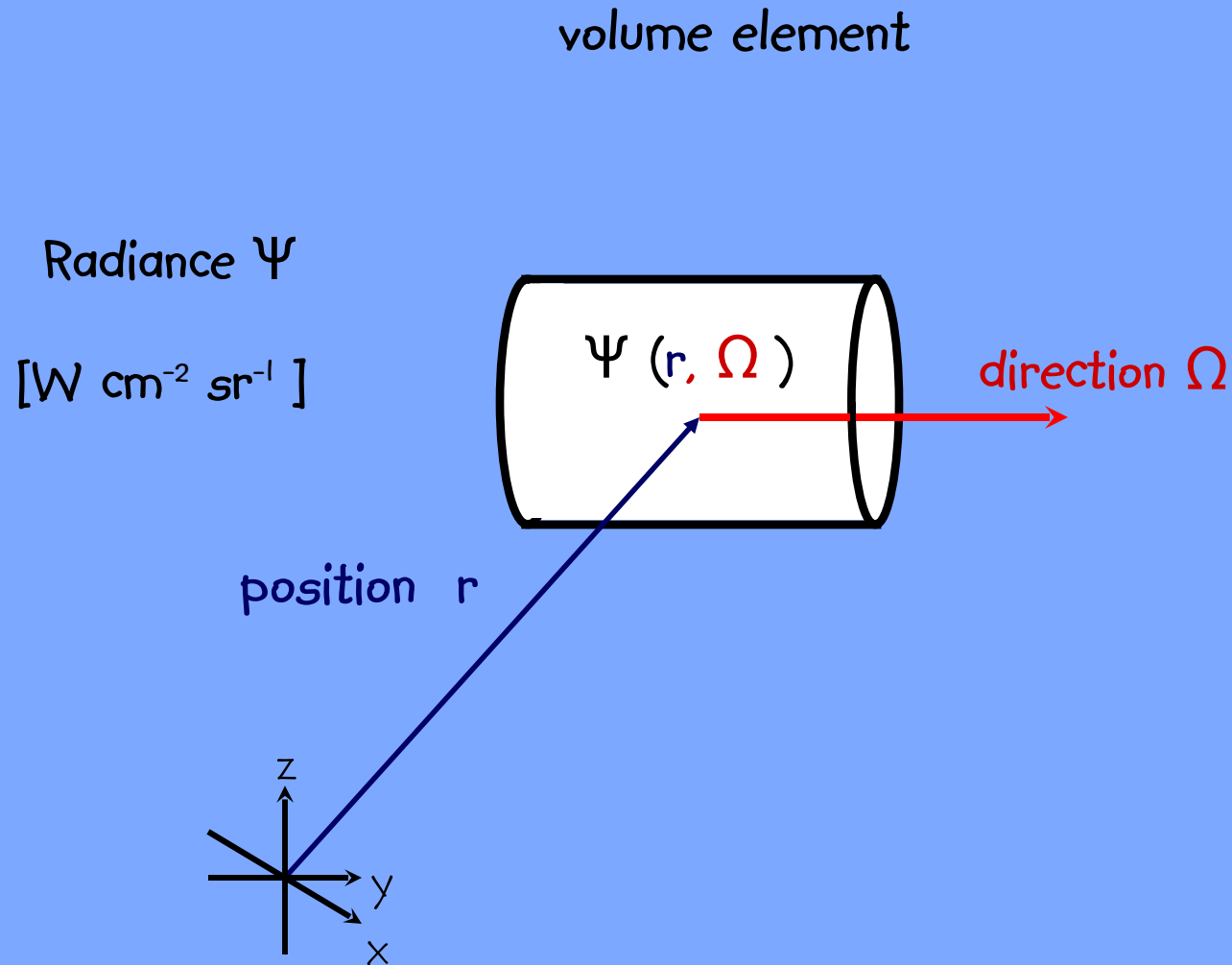
Forward Model

Inverse Model

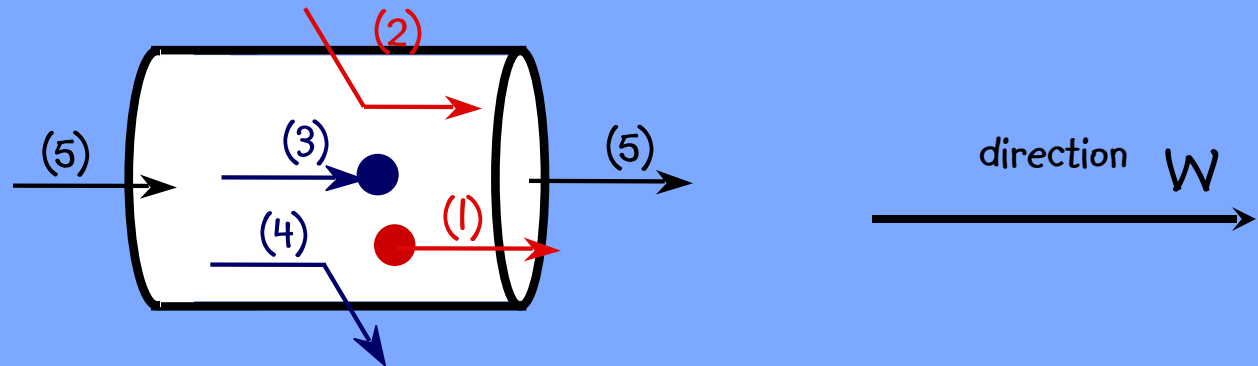
Fluorescence Molecular Tomography

Bioluminescence Tomography

Radiative Transfer Model



Radiative Transfer Model



(1) gain - source

(3) loss - absorption

(2) gain - scattering

(4) loss - scattering

(5) loss / gain - stream

$$\underbrace{\Omega \cdot \nabla \psi(r, \Omega)}_{(5)} + \underbrace{\mu_t \psi(r, \Omega)}_{(3+4)} = \underbrace{Q(r)}_{(1)} + \underbrace{\mu_s \int_{4\pi} p(\Omega, \Omega') \psi(r, \Omega') d\Omega'}_{(2)}$$

balance equation



Radiative Transfer Model

transport equation:

$$\Omega \cdot \nabla \psi(r, \Omega) + \mu_t \psi(r, \Omega) = Q(r) + \mu_s \int_{4\pi} p(\Omega, \Omega') \psi(r, \Omega') d\Omega'$$

attenuation coefficient:

$$\mu_t = \mu_a + \mu_s$$

partial-reflective boundary condition:

$$\psi(\Omega) = R(\Omega' \cdot n) \psi(\Omega') + S(\Omega) \quad \text{for } \Omega \cdot n < 0$$

partial current at boundary:

$$J = \int_{\Omega \cdot n > 0} (n \cdot \Omega) \psi d\Omega$$

flux (fluence):

$$\Phi = \int_{4\pi} \psi(\Omega) d\Omega$$



Radiative Transfer Model - Approximations

Diffusion Equation:

$$-\nabla \cdot \frac{l}{3\mu_{d1}} \nabla \phi_1 + \mu_a \phi_1 = Q$$

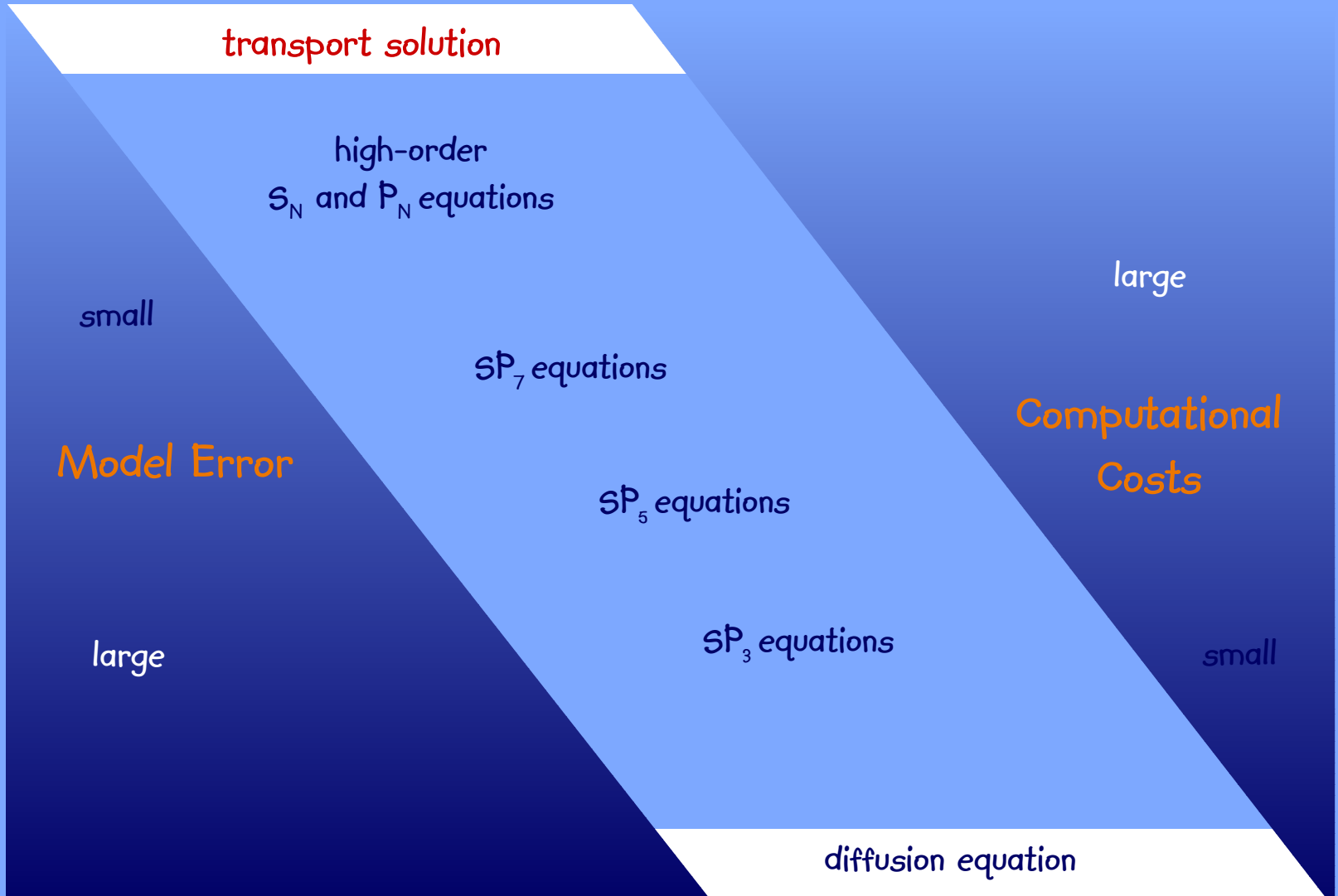
SP₃ Equations:

$$-\nabla \cdot \frac{l}{3\mu_{d1}} \nabla \phi_1 + \mu_a \phi_1 = Q + \left(\frac{3}{2}\mu_a\right) \phi_2$$

$$-\nabla \cdot \frac{l}{7\mu_{d3}} \nabla \phi_2 + \left(\frac{4}{9}\mu_a + \frac{5}{9}\mu_{a2}\right) \phi_2 = -\frac{2}{3}Q + \left(\frac{3}{2}\mu_a\right) \phi_1$$



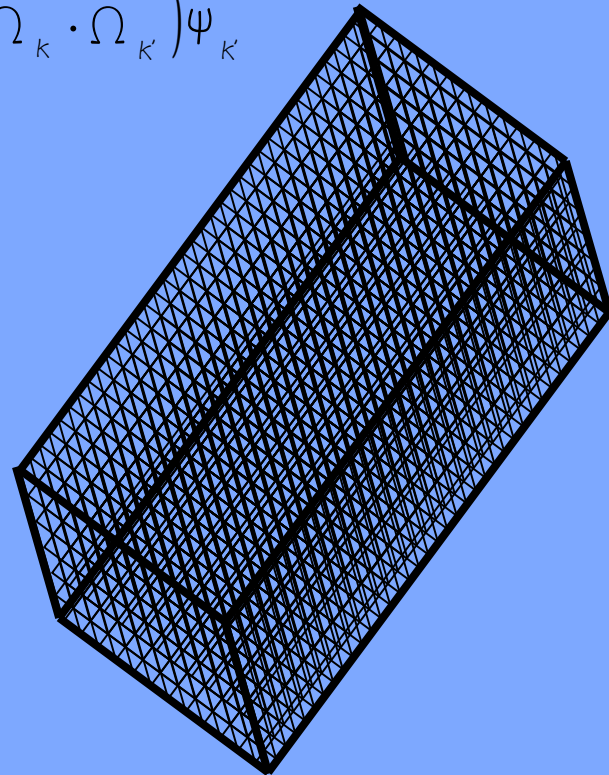
Radiative Transfer Models - Benefits vs. Costs



Finite-Difference Discrete-Ordinates (S_N)

$$\Omega_k \cdot \delta_k \psi_k + (\mu_a + \mu_s) \psi_k = Q_k + \mu_s \sum_{k'} w_{kk'} (\Omega_k \cdot \Omega_{k'}) \psi_{k'}$$

- Upwind FD
- S_8 and 40x40x80 grid
- 10 Million coupled equations
- Source Iteration
(Gauss-Seidel, SOR, etc.)



3D Cartesian grid



Overview

Forward Model

Inverse Model

Fluorescence Molecular Tomography

Bioluminescence Tomography



Inverse Problems

Non-Optical

- X-Ray Computed Tomography (CT)
- Positron Emission Tomography (PET)
- Single Photon Emission Computed Tomography (SPECT)

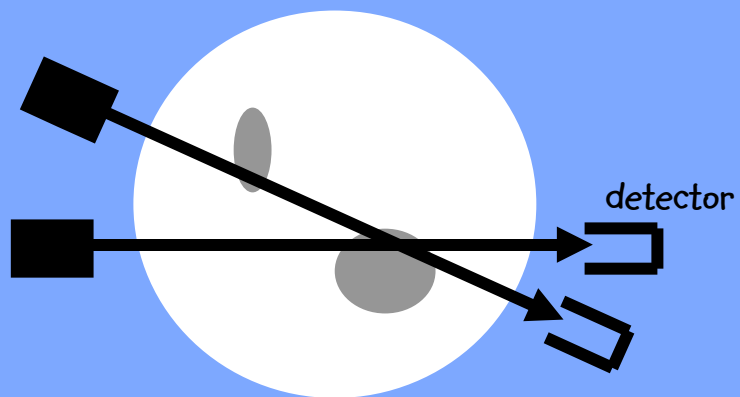
Optical

Diffuse Optical Tomography (DOT)

- Fluorescence Molecular Tomography (FMT)
- Bioluminescence Tomography (BLT)
-

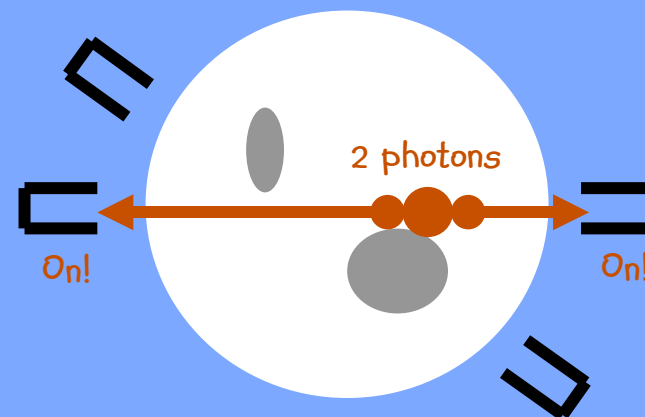
Inverse Problems - Non-Optical

X-Ray CT



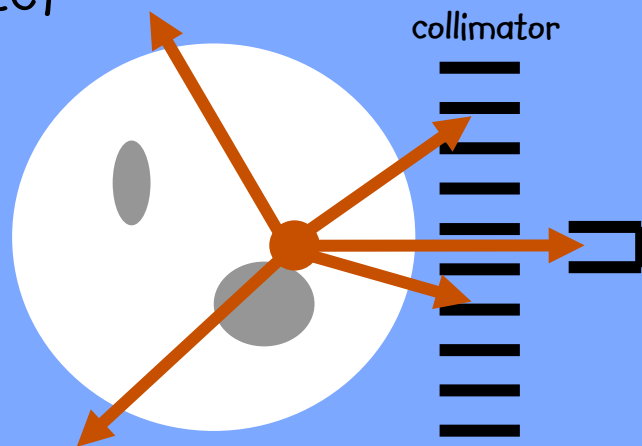
10-100 keV

PET



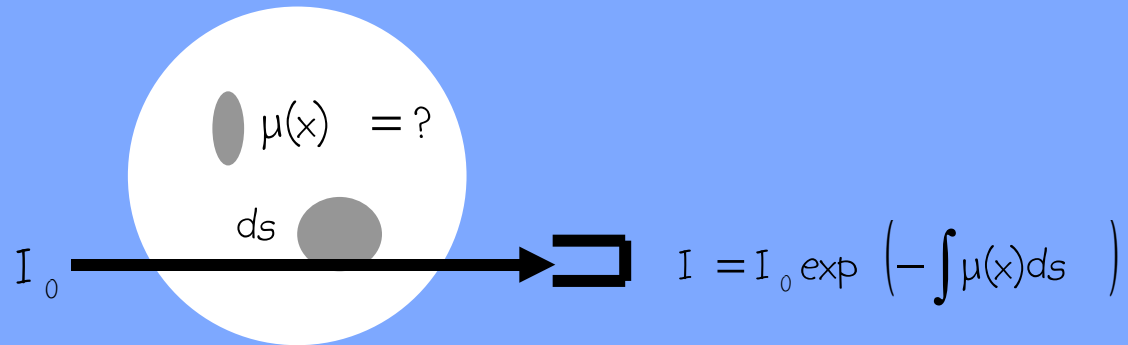
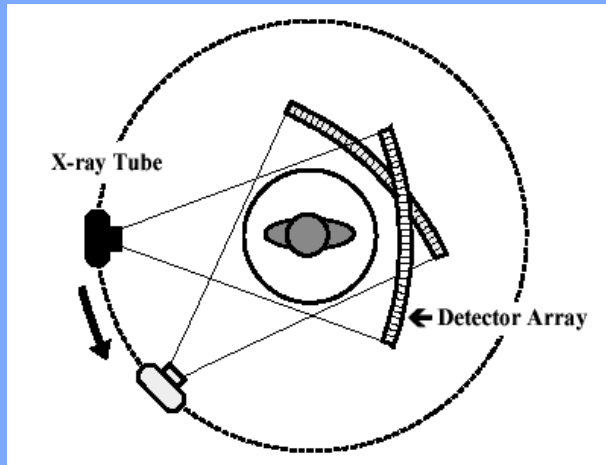
511 keV

SPECT



27-245 keV

Inverse Problems – Non-Optical



Radon Transform

$$g = \ln(I_0/I) = \int \mu(x) ds$$

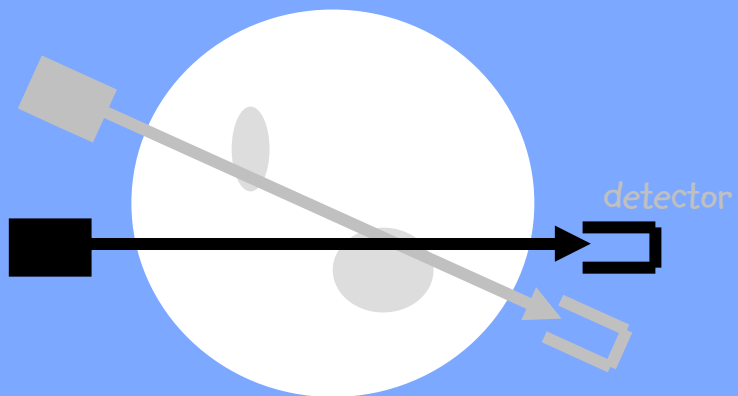
$$g = \mathcal{R}\mu$$

Inverse Radon Transform

$$\mu = \mathcal{R}^{-1} g$$

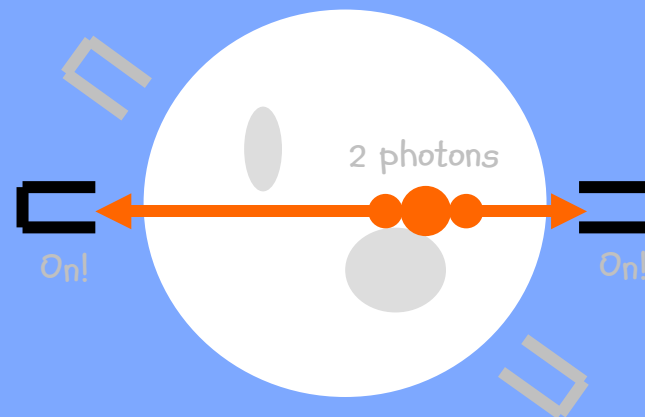
Inverse Problems - Optical

X-Ray CT



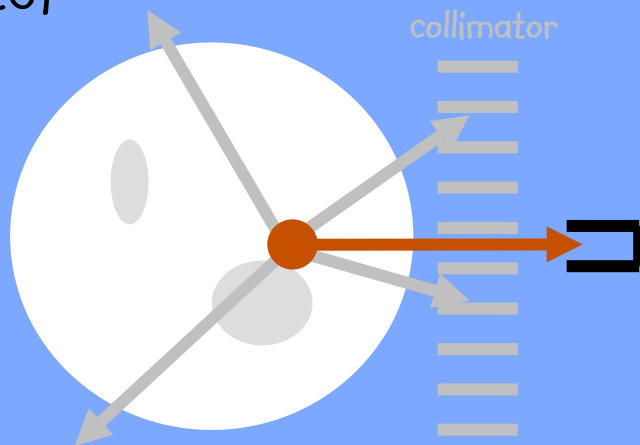
10-100 keV

PET



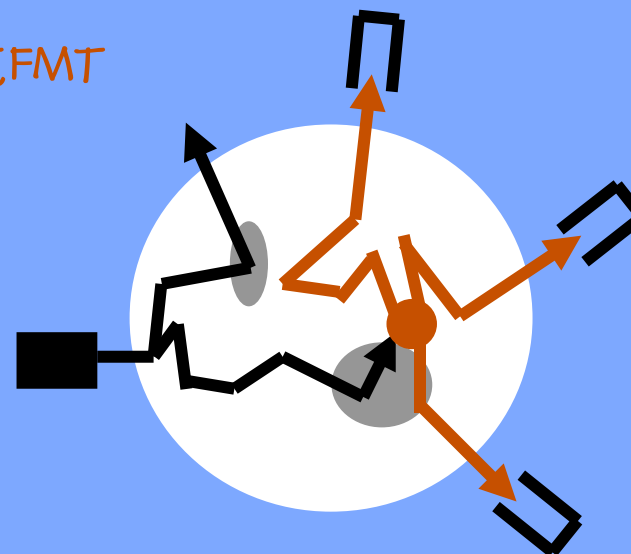
511 keV

SPECT



27-245 keV

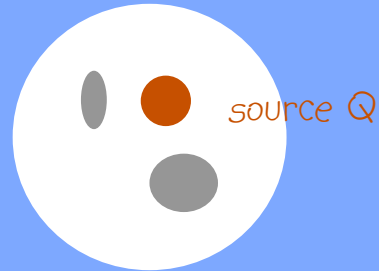
BLT, FMT



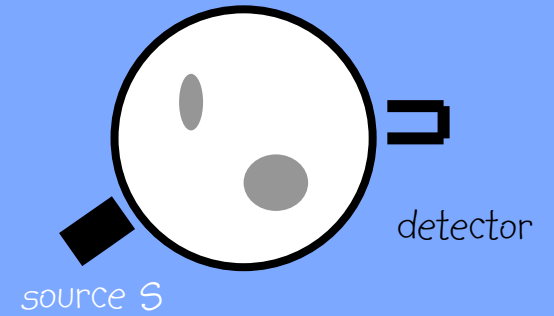
1-3 eV

Inverse Problems – Radiative Transfer

inside of medium



boundary of medium



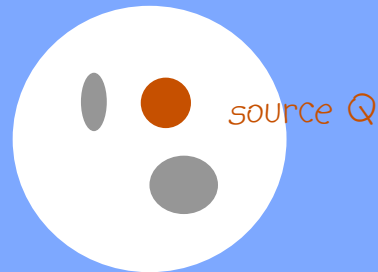
X-Ray CT

PET
SPECT

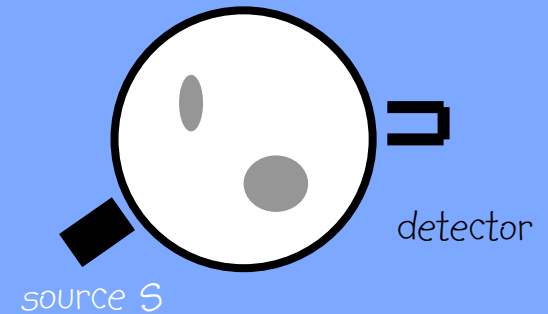
BLT
FMT

Inverse Problems – Radiative Transfer

inside of medium



boundary of medium



X-Ray CT

$$\Omega \cdot \nabla \psi + \sigma_t \psi = 0$$

$$\psi = S, \quad n \cdot \Omega < 0$$

PET
SPECT

$$\Omega \cdot \nabla \psi + \sigma_t \psi = Q$$

$$\psi = 0, \quad n \cdot \Omega < 0$$

BLT
FMT

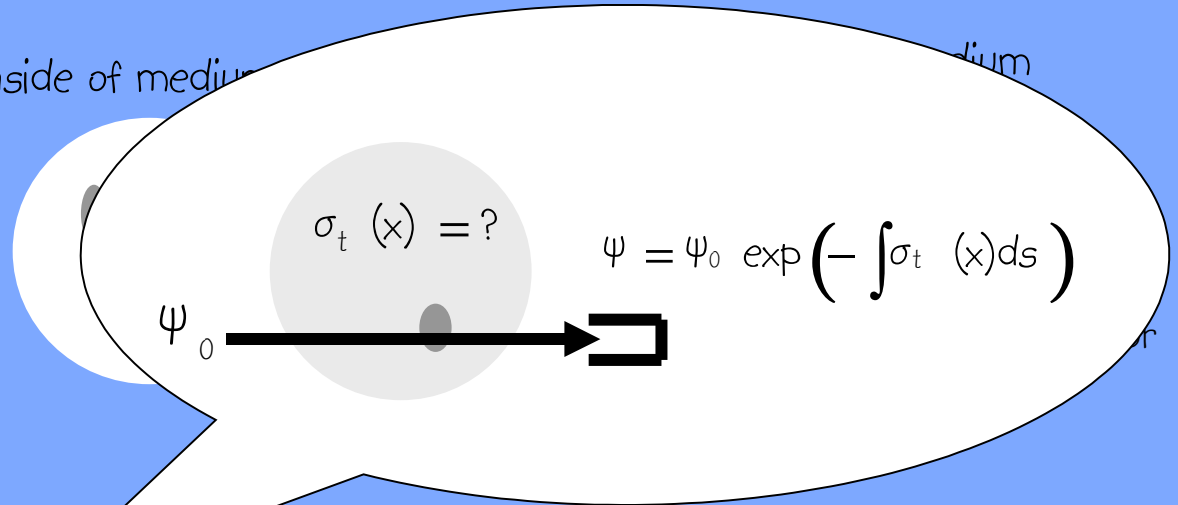
$$\Omega \cdot \nabla \psi + \sigma_t \psi = Q + \sigma_s \int_{4\pi} p(\Omega \cdot \Omega') \psi d\Omega'$$

$$\psi = S, \quad n \cdot \Omega < 0$$

Inverse Problems – Radiative Transfer

inside of medium

medium



X-Ray CT

$$\Omega \cdot \nabla \psi + \sigma_t \psi = 0$$

$$\psi = \mathcal{S}, \quad n \cdot \Omega < 0$$

PET
SPECT

$$\Omega \cdot \nabla \psi + \sigma_t \psi = \mathcal{Q}$$

?

$$n \cdot \Omega < 0$$

BLT
FMT

$$\Omega \cdot \nabla \psi + \sigma_t \psi = \mathcal{Q} + \sigma_s \int_{4\pi} p(\Omega \cdot \Omega') \psi d\Omega'$$

$$\psi = \mathcal{S}, \quad n \cdot \Omega < 0$$



Overview

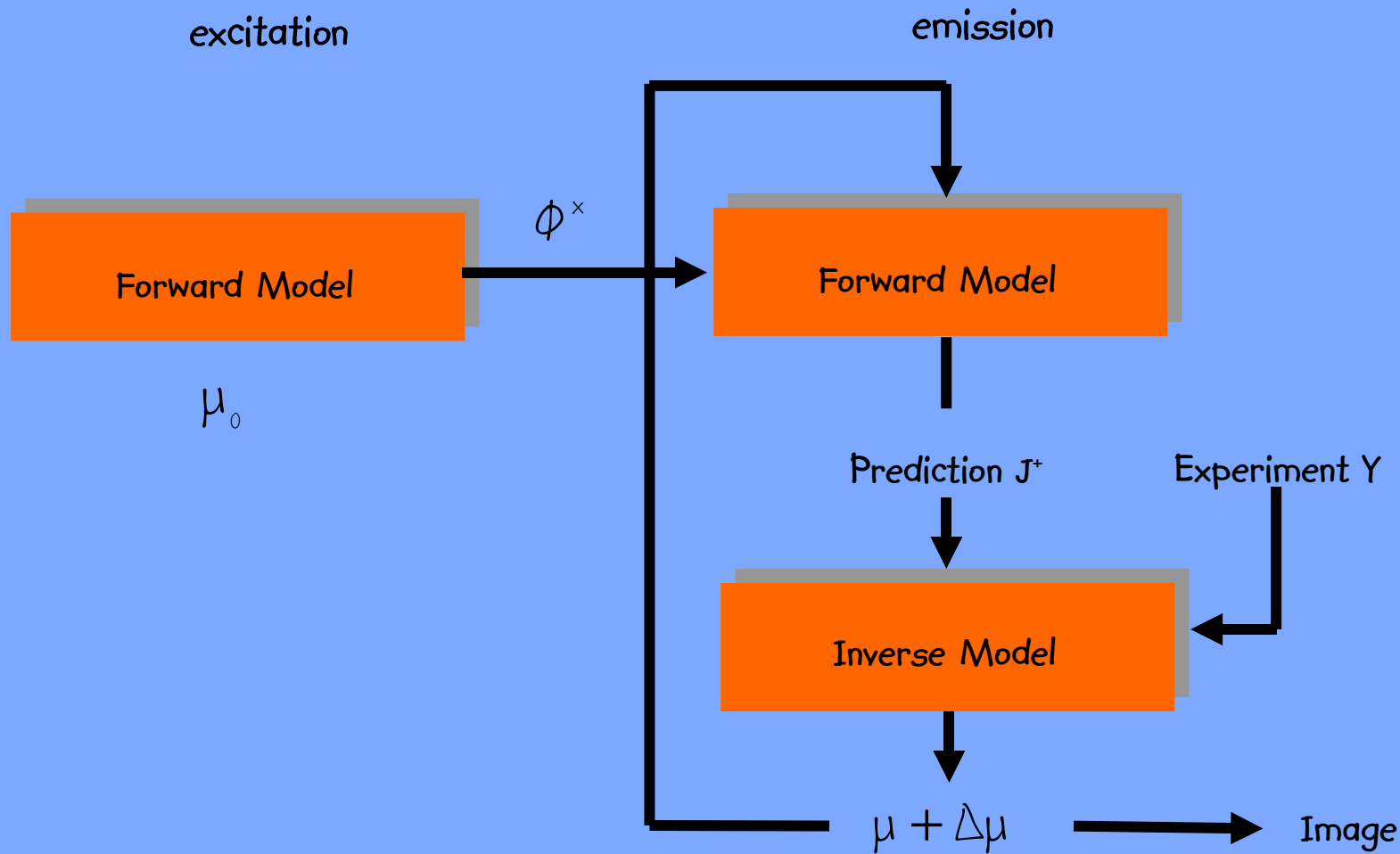
Forward Model

Inverse Model

Fluorescence Molecular Tomography

Bioluminescence Tomography

Fluorescence Molecular Tomography

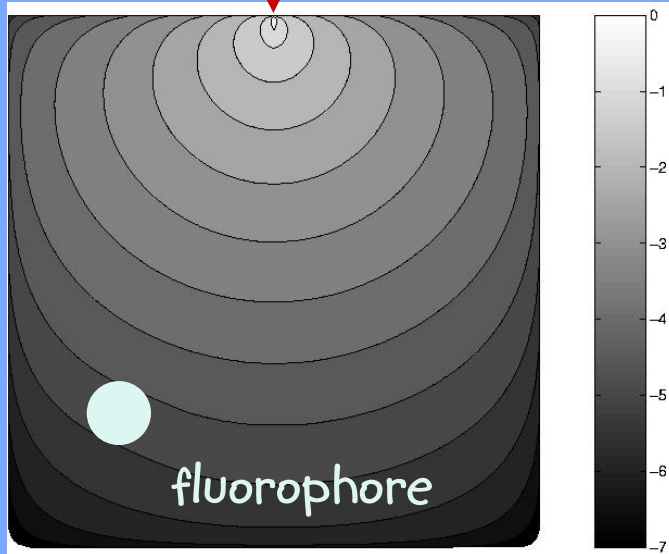


Radiative Transfer Model - Fluorescence

excitation

$$\phi^x$$

[W cm⁻²]



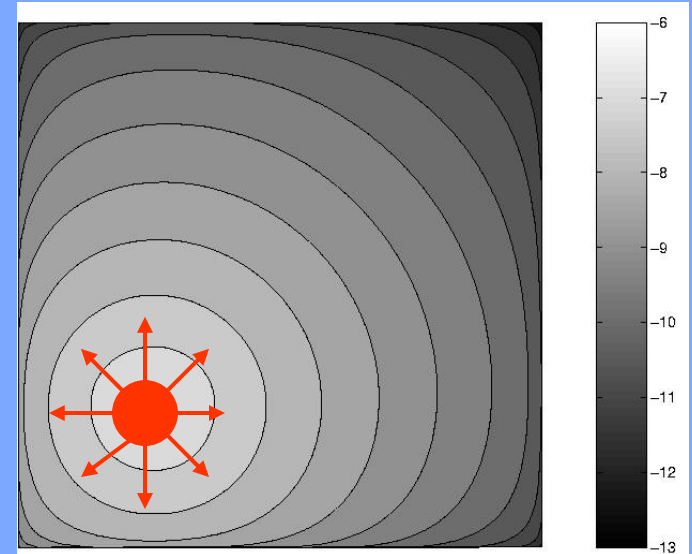
light absorption by fluorophore

$$\mu_a^{x \rightarrow m} = c \cdot \epsilon$$

emission

$$\phi^m$$

[W cm⁻²]



light emission by fluorophore

$$Q^m = \frac{1}{4\pi} \eta \mu_a^{x \rightarrow m} \phi^x$$



Radiative Transfer Model - Fluorescence

excitation

$$\Omega \cdot \nabla \psi^x + (\mu_a + \mu_a^{x \rightarrow m} + \mu_s) \psi^x = \mu_s \int_{4\pi} p(\Omega \cdot \Omega') \psi^x d\Omega'$$

$$\psi^x = S, \quad n \cdot \Omega < 0$$

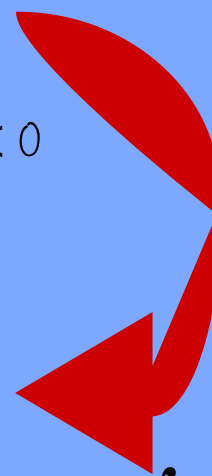
excitation
field

$$\Phi^x = \int_{4\pi} \psi^x d\Omega$$

emission

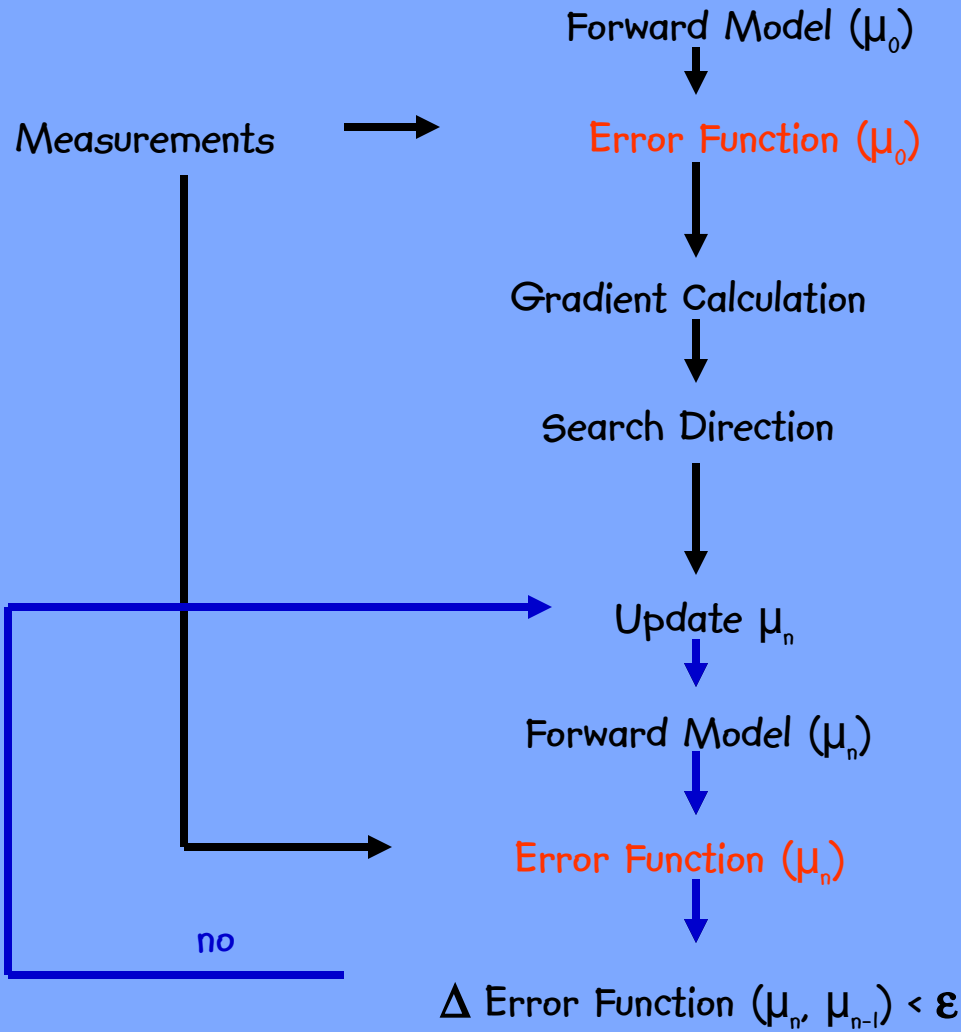
$$\Omega \cdot \nabla \psi^m + (\mu_a + \mu_s) \psi^m = \frac{1}{4\pi} \eta \mu_a^{x \rightarrow m} \Phi^x + \mu_s \int_{4\pi} p(\Omega \cdot \Omega') \psi^m d\Omega'$$

$$\psi^m = 0, \quad n \cdot \Omega < 0$$





Local Optimization

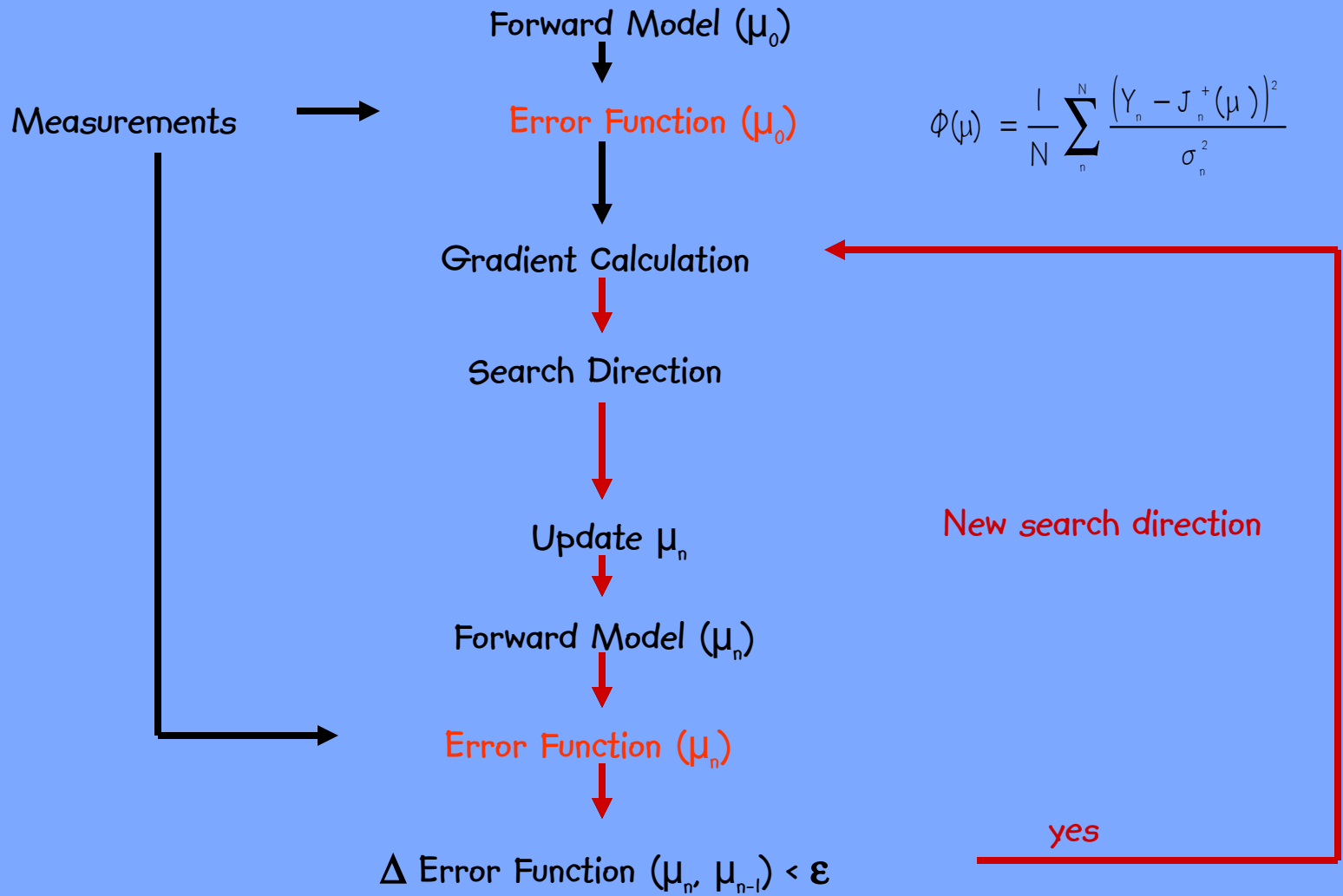


$$\Phi(\mu) = \frac{1}{N} \sum_n \frac{(Y_n - J_n^+(\mu))^2}{\sigma_n^2}$$

Search algorithm



Local Optimization



$$\Phi(\mu) = \frac{1}{N} \sum_n \frac{(Y_n - J_n^+(\mu))^2}{\sigma_n^2}$$



Computation Of Search Direction

$$\frac{\partial \phi}{\partial \mu_a} = \left(\frac{\partial \phi}{\partial \mu_{a1}}, \frac{\partial \phi}{\partial \mu_{a2}}, \dots, \frac{\partial \phi}{\partial \mu_{aN}} \right)$$



amount of image voxels



Adjoint Differentiation

error function Φ is split up into subfunctions given Ψ^z by the radiative transfer model

$$\Phi(\mu) = \left(\tilde{\Phi} \circ \Psi^z \circ \dots \circ \Psi^{z+1} \circ \Psi^z \circ \dots \circ \Psi^2 \circ \Psi^1 \right) (\mu)$$

source iteration:
(sub-functions)

$$A \Psi^0 = Q$$

$$A \Psi^1 = B \Psi^0 + Q$$

$$A \Psi^2 = B \Psi^1 + Q$$

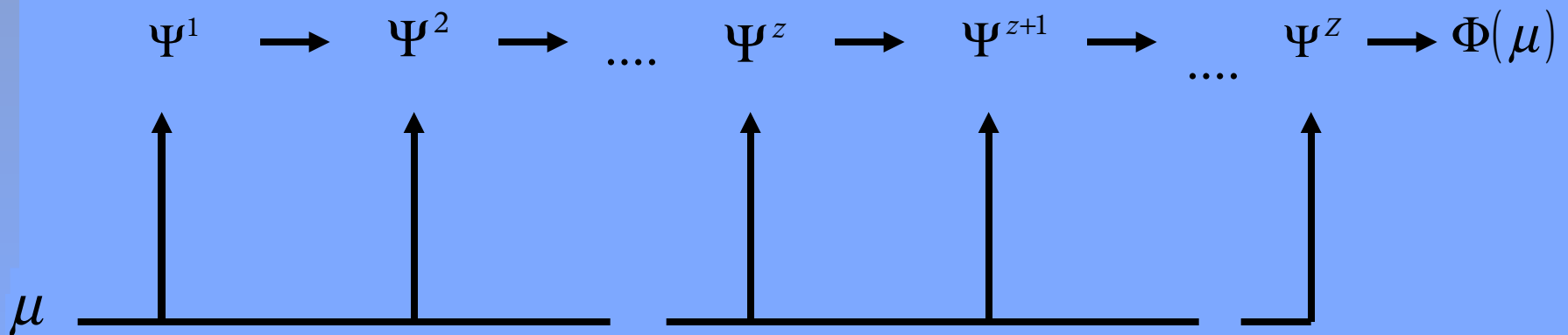


Adjoint Differentiation

error function Φ is split up into subfunctions given Ψ^z by the radiative transfer model

$$\Phi(\mu) = \left(\tilde{\Phi} \circ \Psi^z \circ \dots \circ \Psi^{z+1} \circ \Psi^z \circ \dots \circ \Psi^2 \circ \Psi^1 \right) (\mu)$$

forward direction





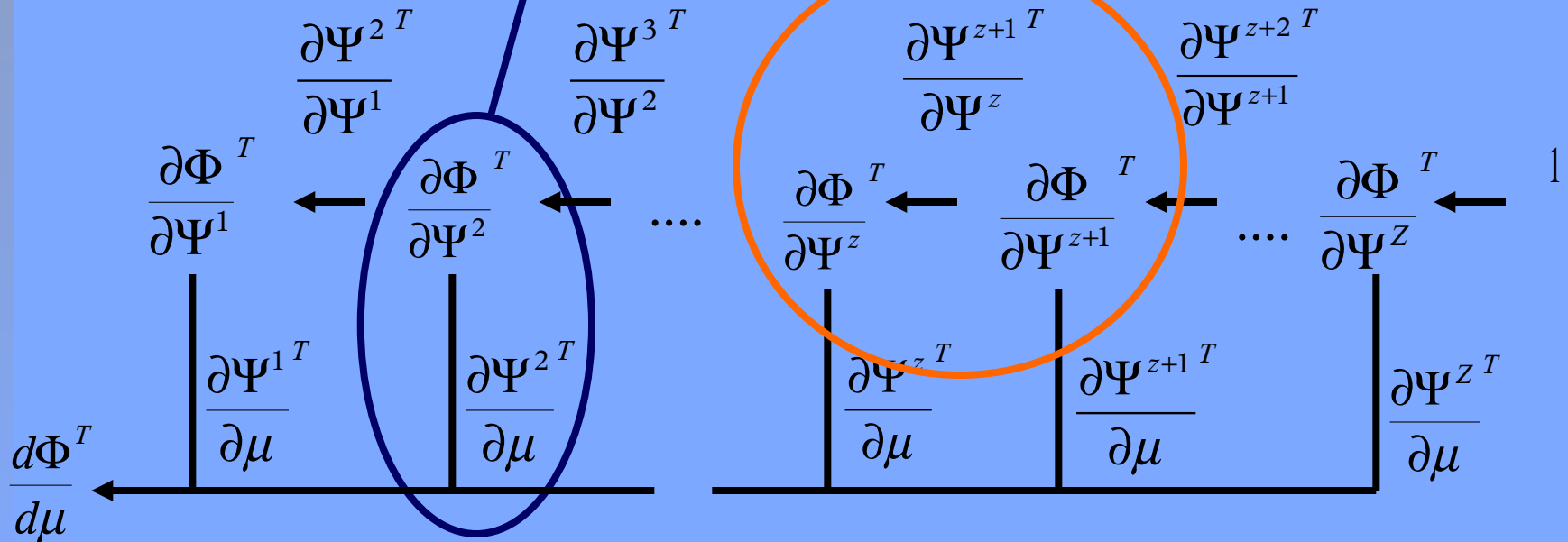
Adjoint Differentiation

chain rule of differentiation

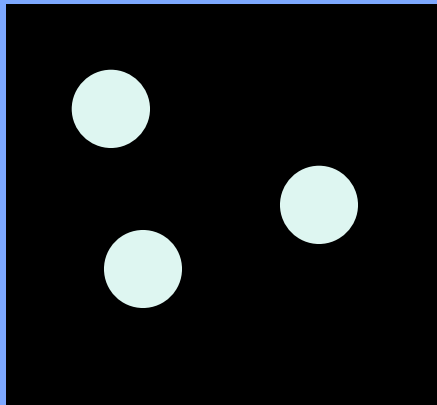
$$\frac{d\Phi^T}{d\mu} = \sum_z \frac{\partial \Psi^z{}^T}{\partial \mu} \frac{\partial \Phi^T}{\partial \Psi^z}$$

$$\frac{\partial \Phi^T}{\partial \Psi^z} = \frac{\partial \Psi^{z+1}{}^T}{\partial \Psi^z} \frac{\partial \Phi^T}{\partial \Psi^{z+1}}$$

reverse direction



Phantom Experiment



3 cm

1) Excitation

solid phantom:

$$\mu_s = 11.6 \text{ cm}^{-1}$$

$$\mu_a = 0.01 \text{ cm}^{-1}$$

fluorophore:

$$\eta = 0.06$$

$$\mu_a^{x-m} = 0.013 \text{ cm}^{-1}$$

wavelength:

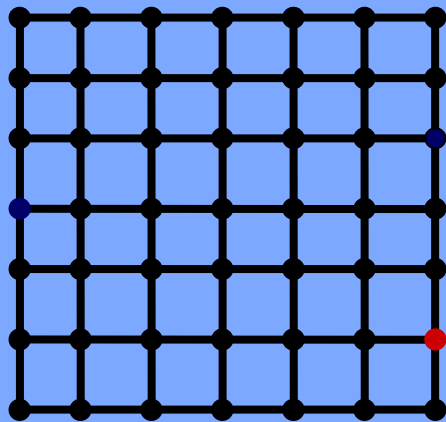
$$\lambda^x = 740 \text{ nm}$$

$$\lambda^m = 802 \text{ nm}$$

Phantom Experiment

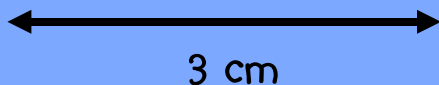
24 discrete ordinates

61 x 61 grid points



4 sources

88 detectors



3 cm

1) Excitation

solid phantom:

$$\mu_s = 11.6 \text{ cm}^{-1}$$

$$\mu_a = 0.01 \text{ cm}^{-1}$$

fluorophore:

$$\eta = 0.06$$

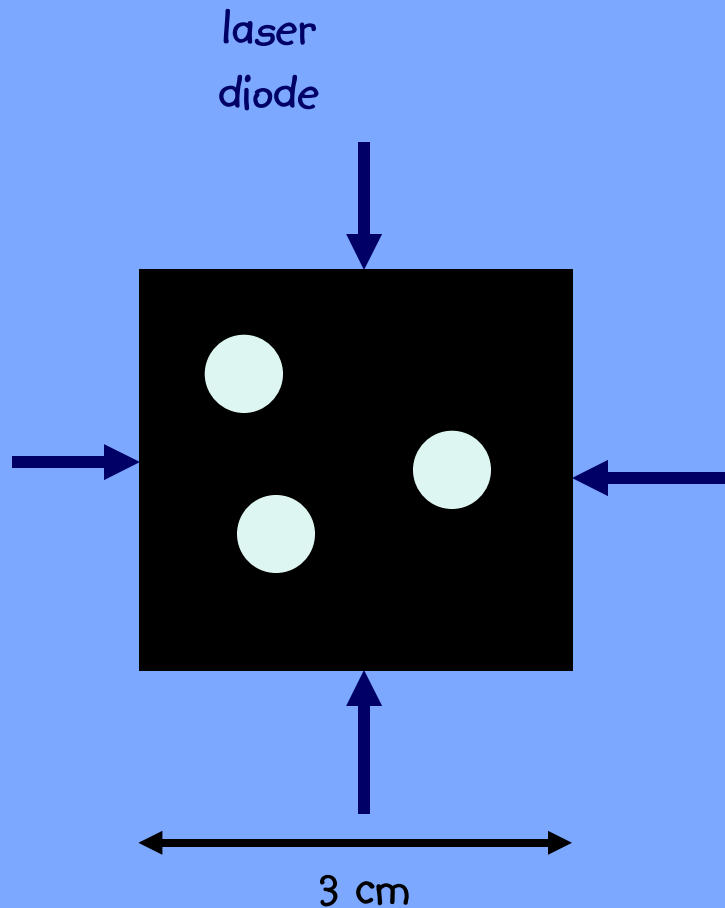
$$\mu_a^{x-m} = 0.013 \text{ cm}^{-1}$$

wavelength:

$$\lambda^x = 740 \text{ nm}$$

$$\lambda^m = 802 \text{ nm}$$

Phantom Experiment



1) Excitation

solid phantom:

$$\mu_s = 11.6 \text{ cm}^{-1}$$

$$\mu_a = 0.01 \text{ cm}^{-1}$$

fluorophore:

$$\eta = 0.06$$

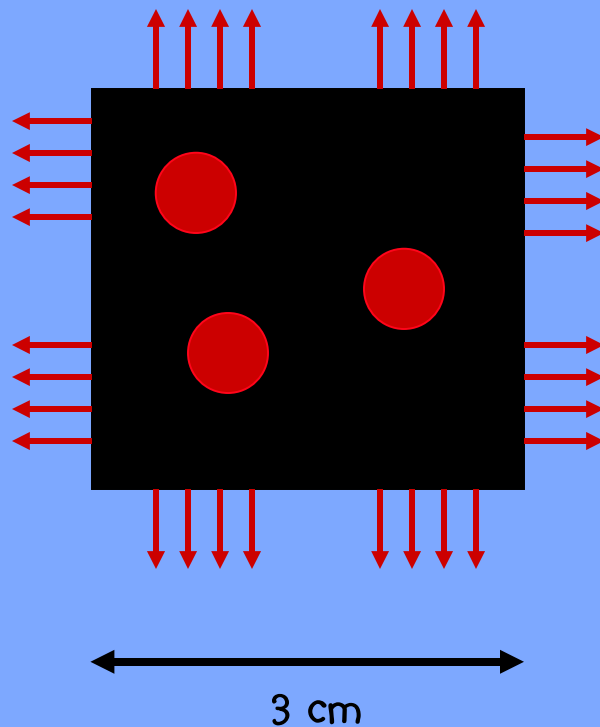
$$\mu_a^{x-m} = 0.013 \text{ cm}^{-1}$$

wavelength:

$$\lambda^x = 740 \text{ nm}$$

$$\lambda^m = 802 \text{ nm}$$

Phantom Experiment



2) Emission

solid phantom:

$$\mu_s = 11.6 \text{ cm}^{-1}$$

$$\mu_a = 0.01 \text{ cm}^{-1}$$

fluorophore:

$$\eta = 0.06$$

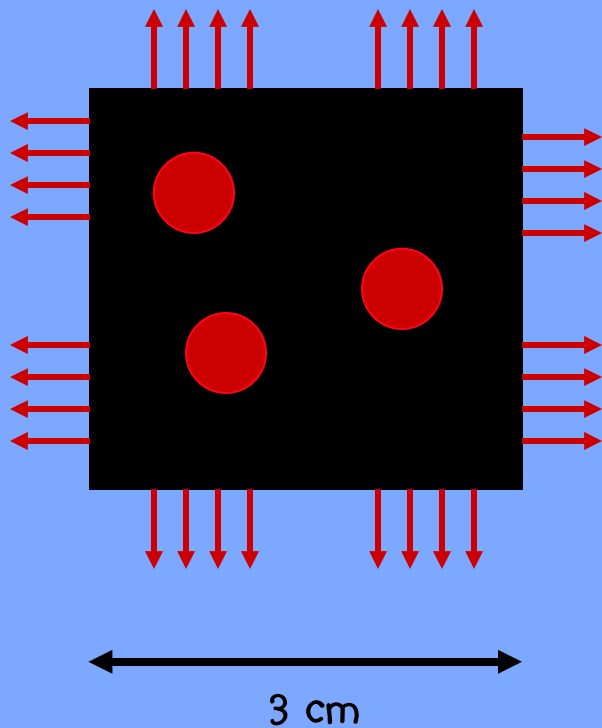
$$\mu_a^{x-m} = 0.013 \text{ cm}^{-1}$$

wavelength:

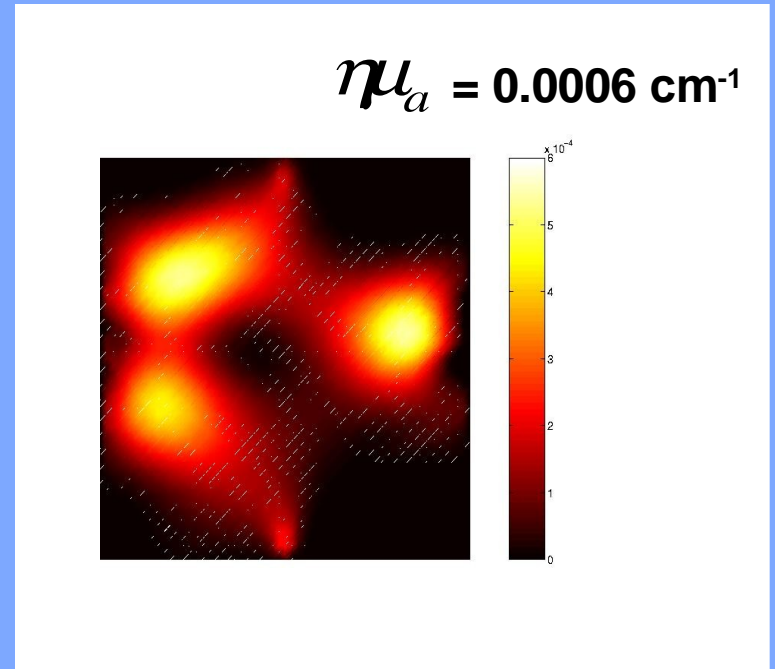
$$\lambda^x = 740 \text{ nm}$$

$$\lambda^m = 802 \text{ nm}$$

Phantom Experiment

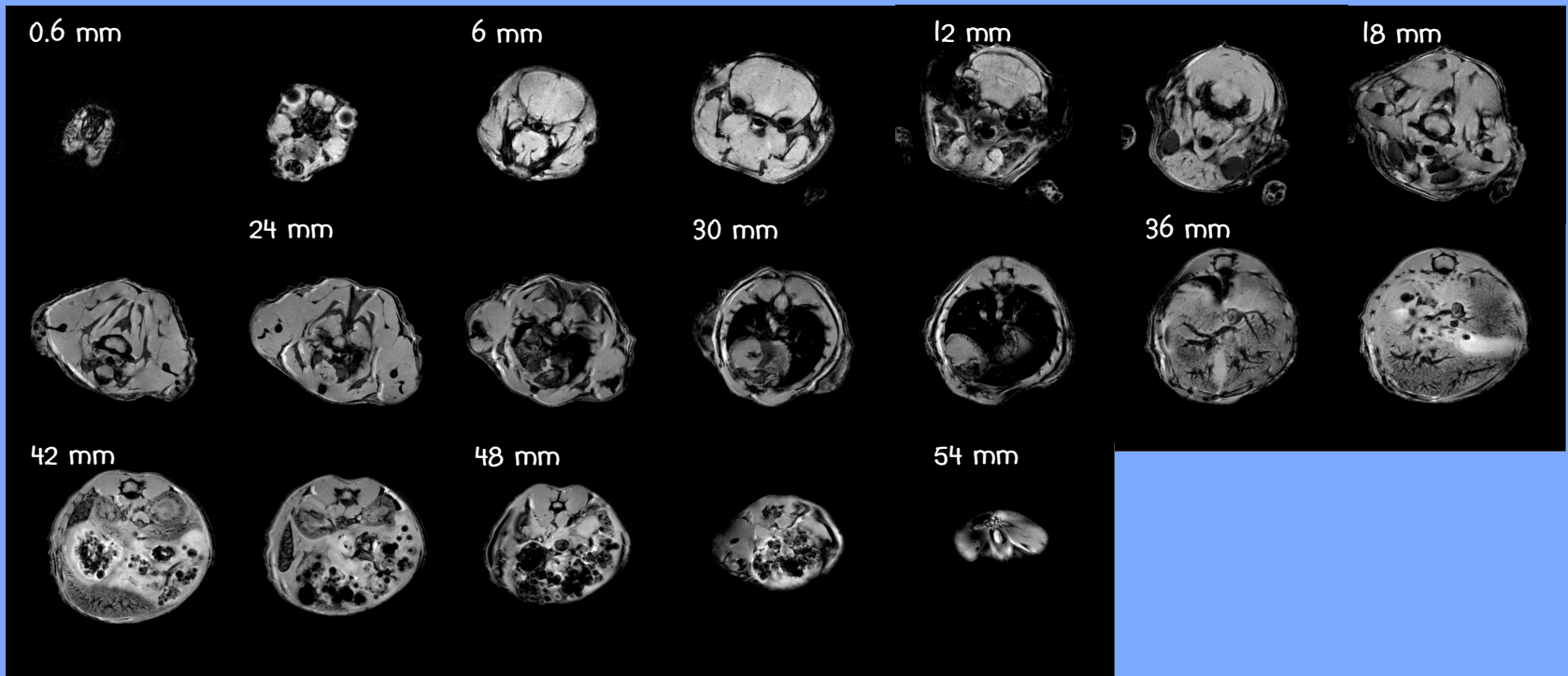


2) Emission



3D Numerical Mouse Model

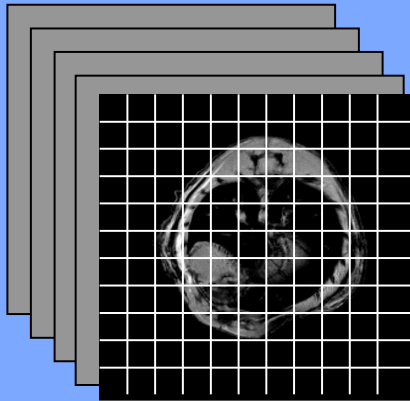
head



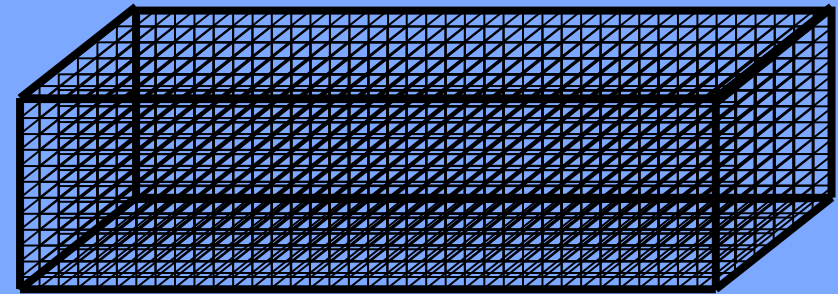
tail

3D Numerical Mouse Model

91 whole-body MRIs
of mouse

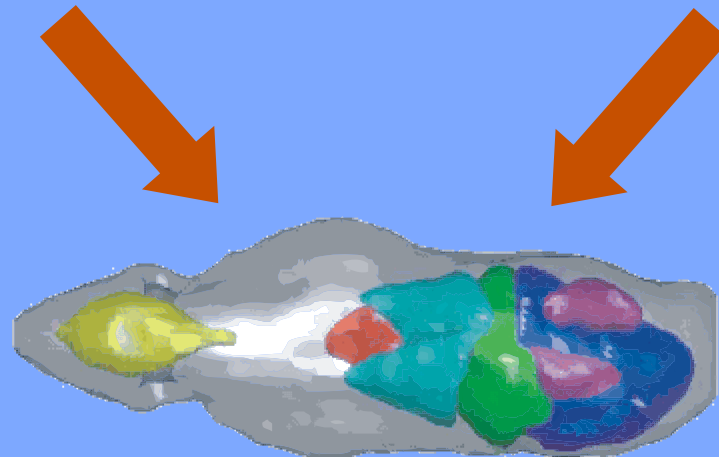


Cartesian grid with
80,000 points



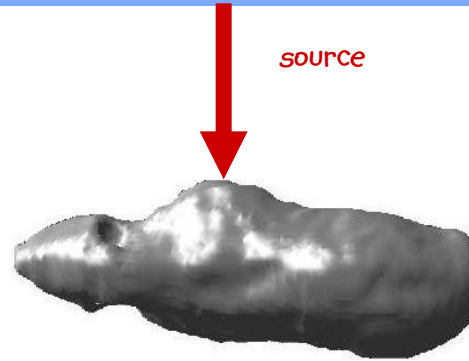
0 mm

54 mm



Numerical Example

excitation



fluorescence



1 cm

1.8 mm³, 400nM Cy5.5

Calculated Boundary Flux

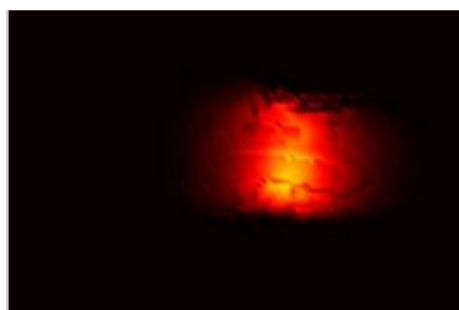
excitation

source



$\log(\text{partial current})$
[Wcm⁻²]

fluorescence

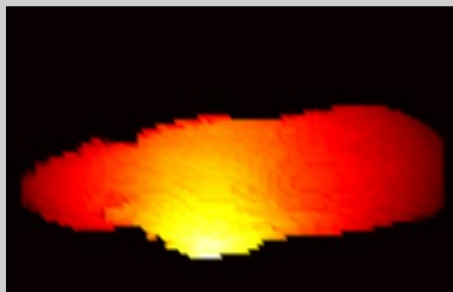


1 cm

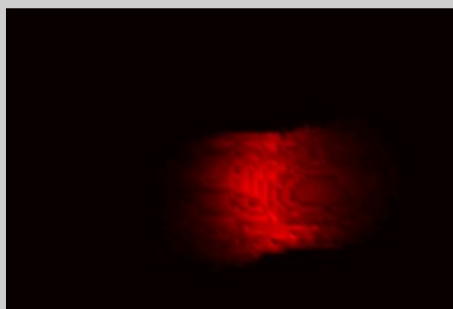
1.8 mm³, 400nM Cy5.5

Calculated Boundary Flux

excitation



fluorescence



log(partial current)

[Wcm⁻²]



-7



-7

Image Reconstruction

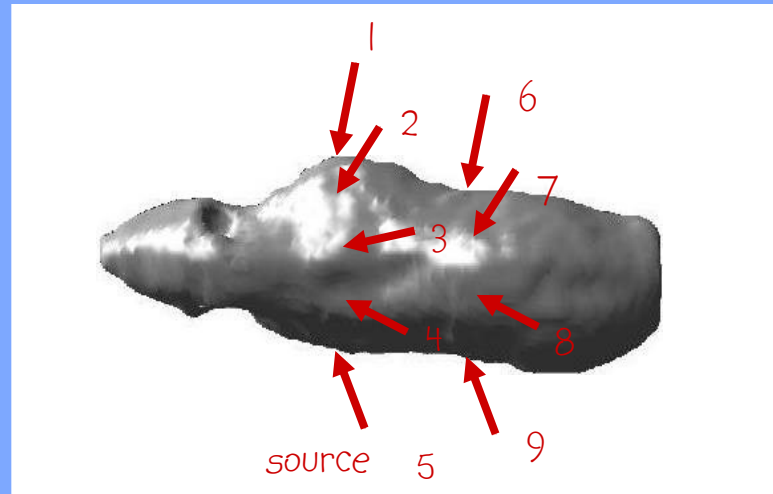
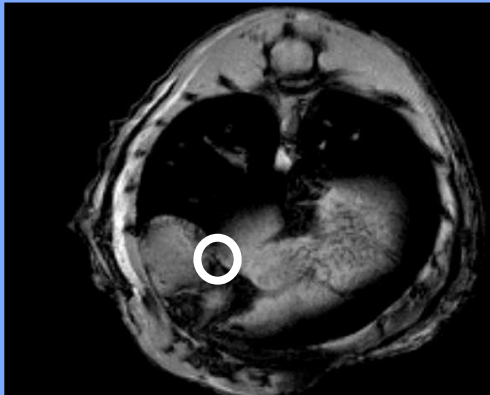


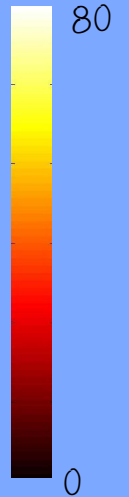
Image Reconstruction

1.8 mm³, 400nM Cy5.5

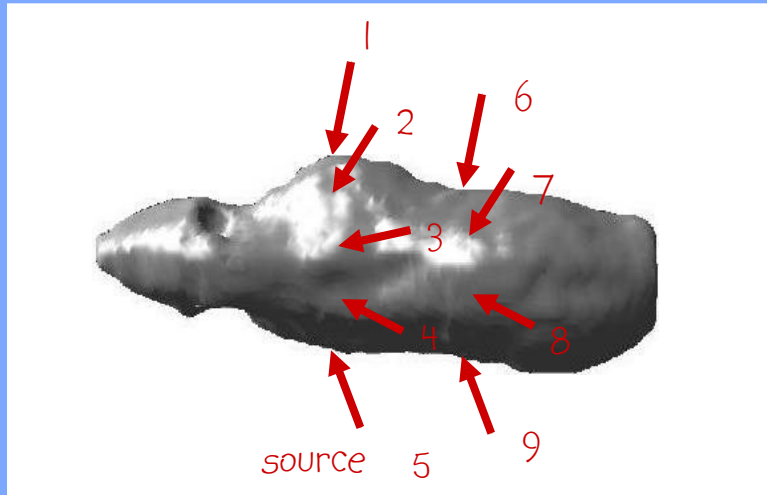


0.5 cm

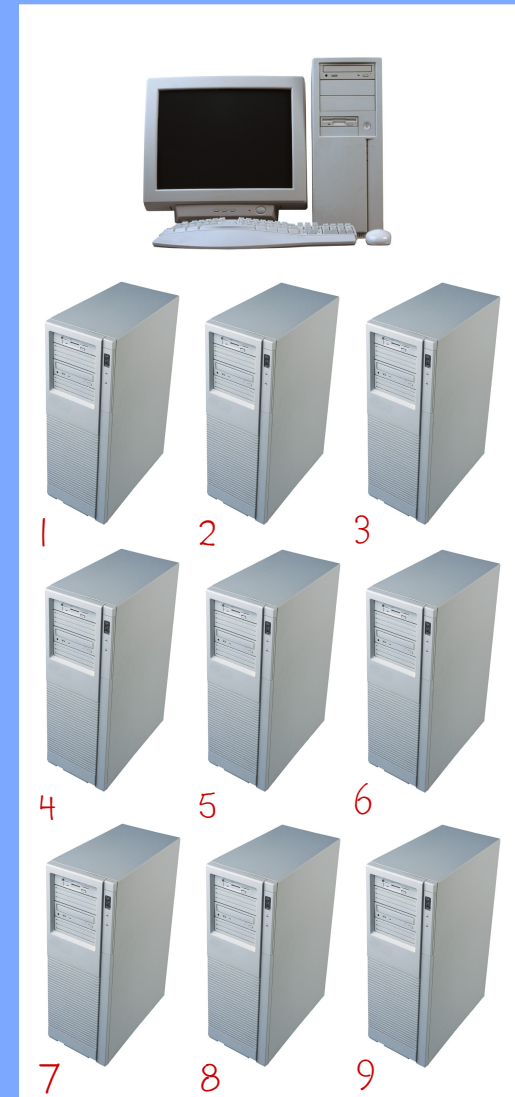
Cy5.5
[nM]



Parallel Computing - Beowulf Cluster

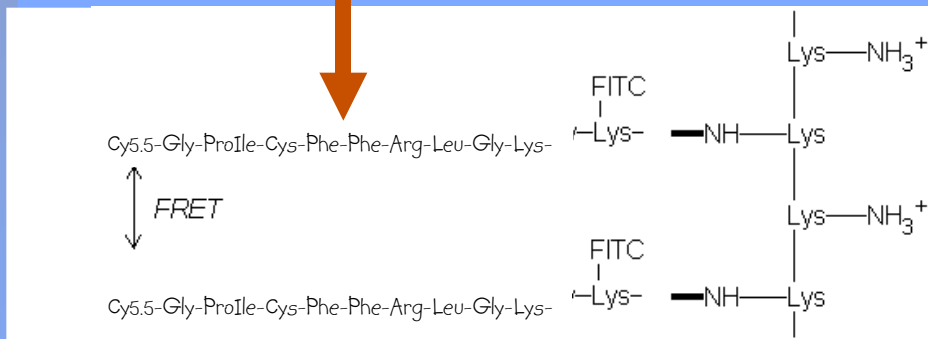
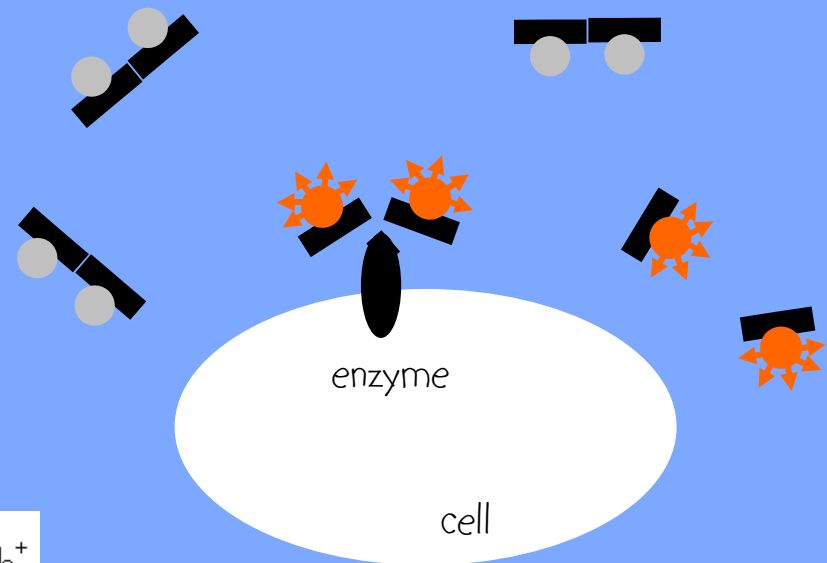
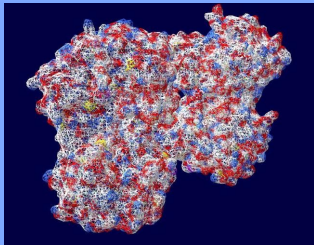


radiative transfer model is solved
for all source positions on # processors



In Vivo Experiments

Fluorescent probe is activated through interaction with a molecular target, e.g. enzyme (Cathepsin D)



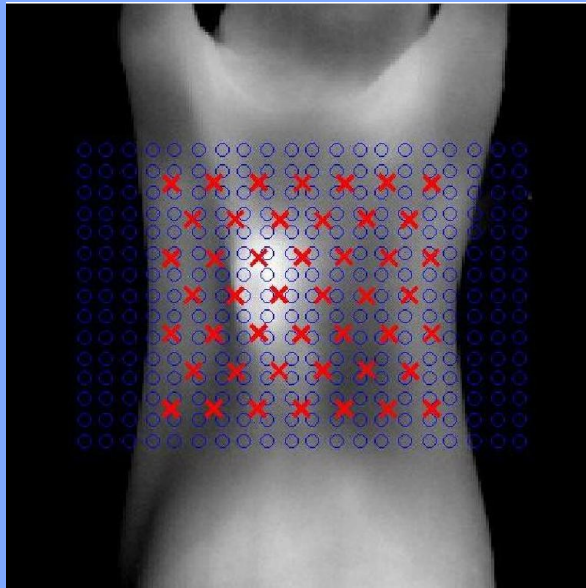
fluorescent probe

Tung et al, Bioconjugate Chemistry 10, (1999)

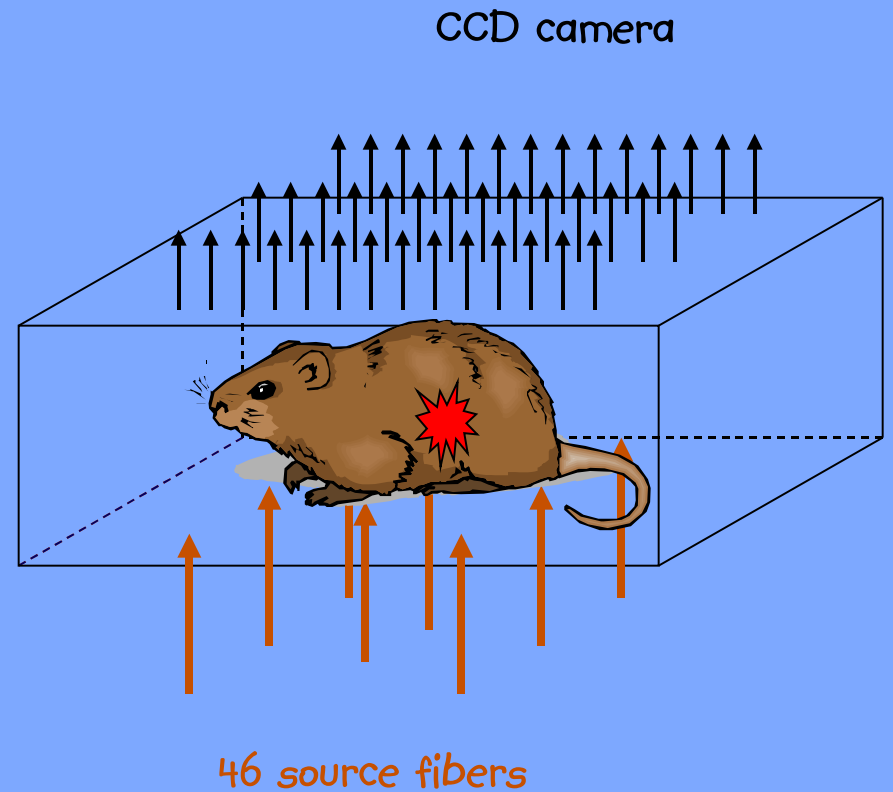
Weissleder et al, Nature Biotechnology 17, (1999)

In Vivo Experiments

Mouse with Lewis Lung Carcinoma (LLC)

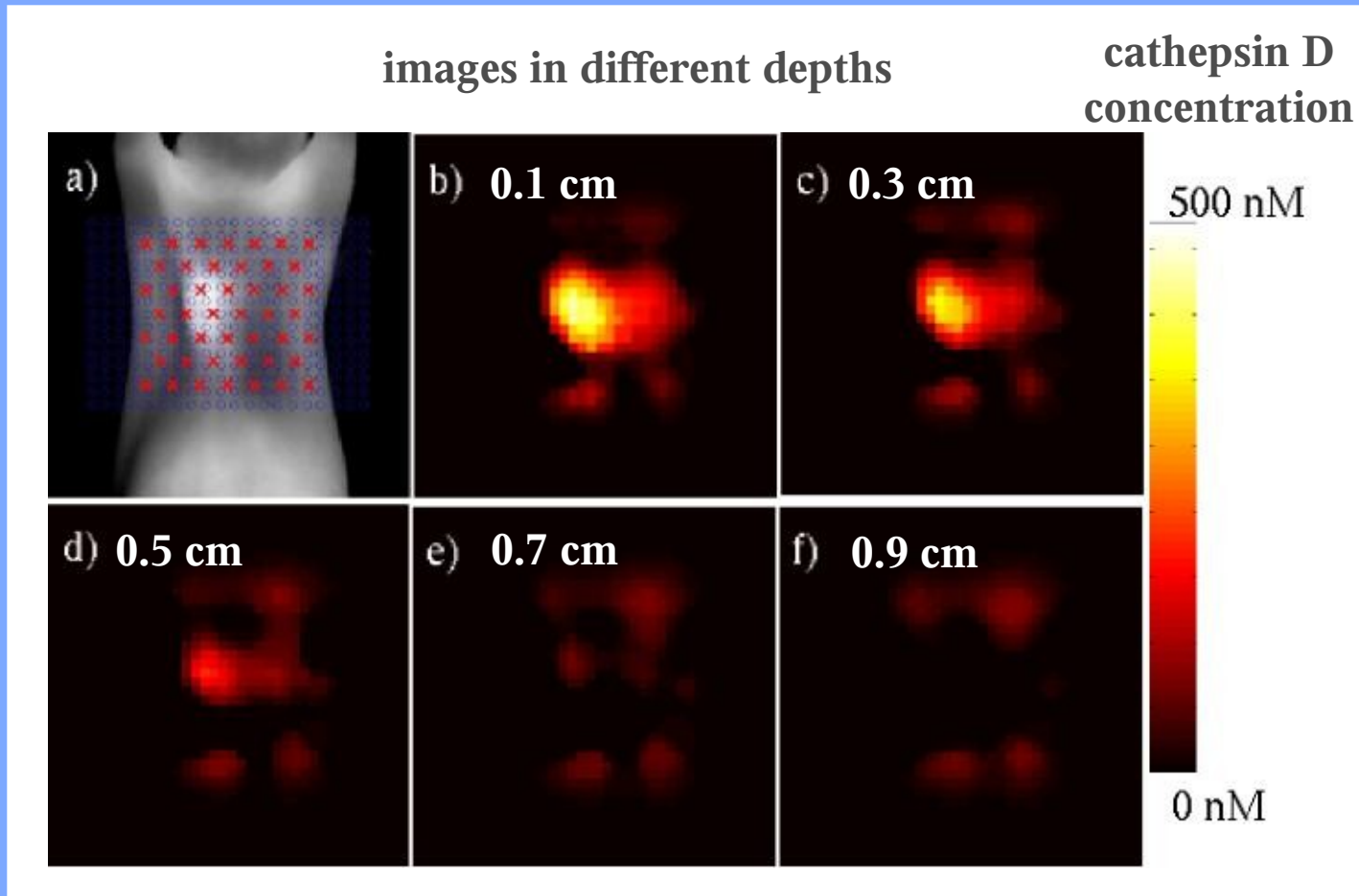


surface-weighted image



Experimental data were provided by V. Ntziachristos, MGH

In Vivo Experiments



Beowulf Cluster

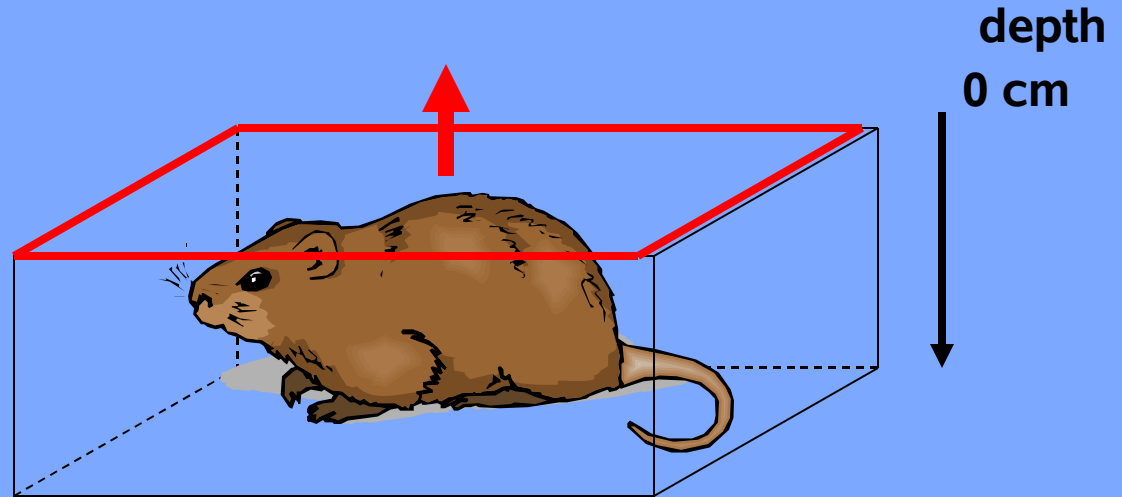


24 CPUs

Parallel Processing (MPI)

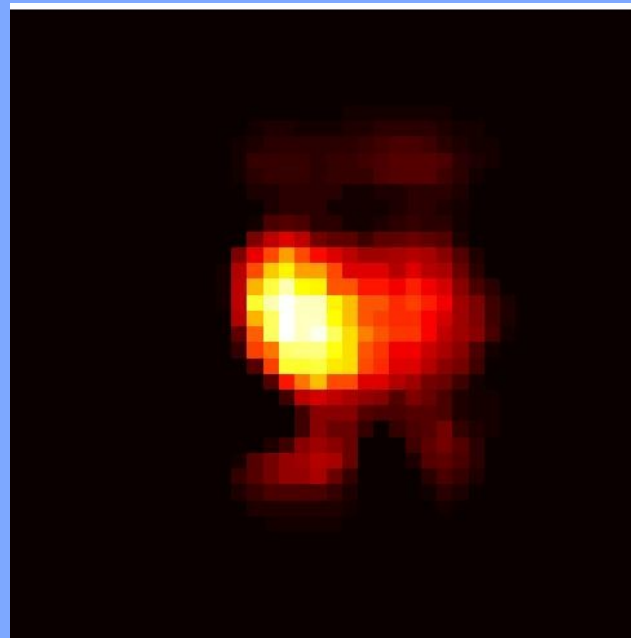
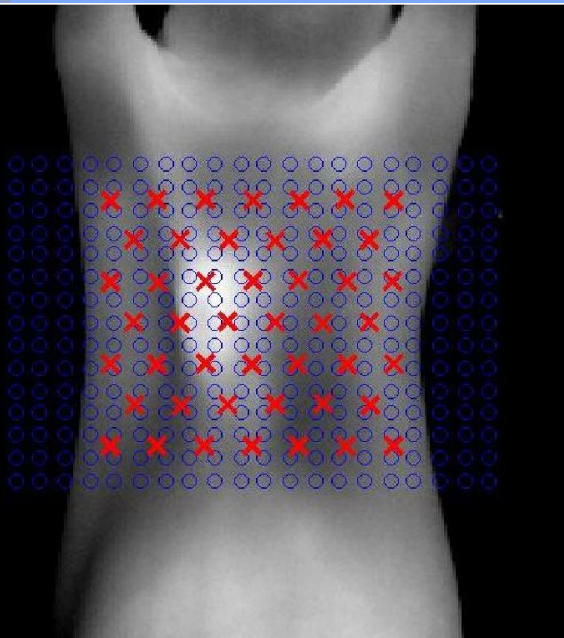
current reconstruction time
3 to 48 hours

In Vivo Experiments



top view

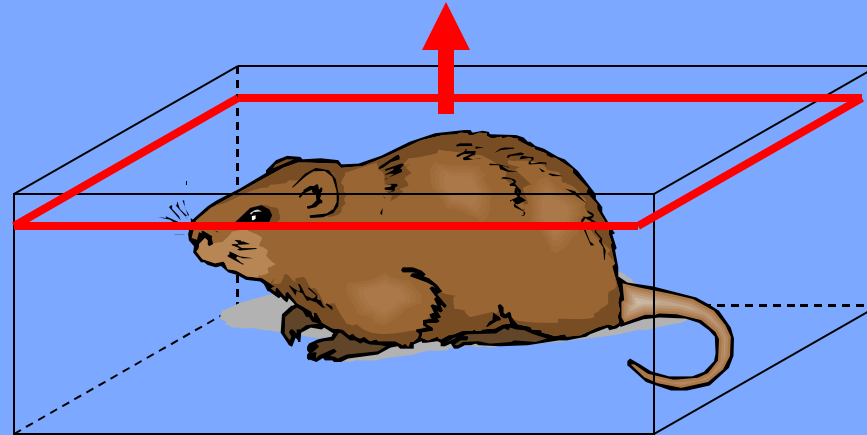
fluorophore
absorption = 0 - 0.032 cm⁻¹



In Vivo Experiments

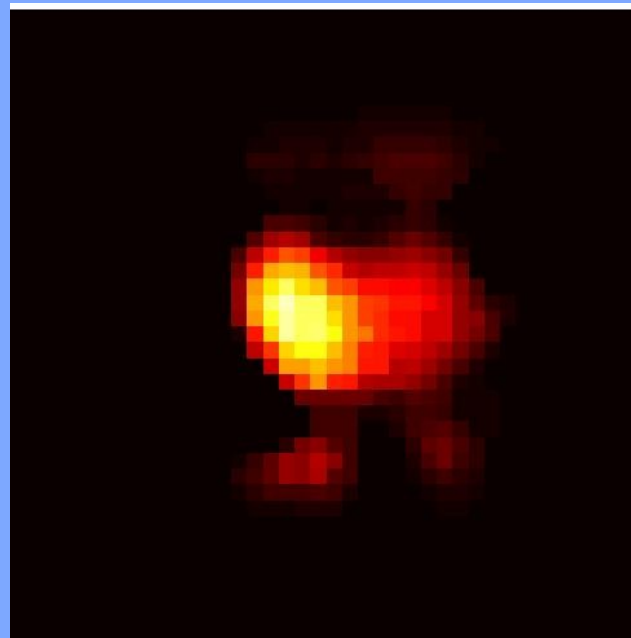
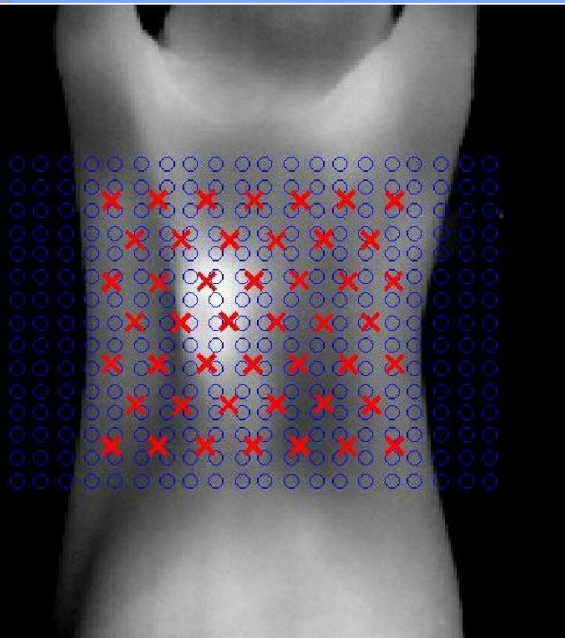
depth

0.1 cm



top view

fluorophore
absorption = 0 - 0.032 cm⁻¹

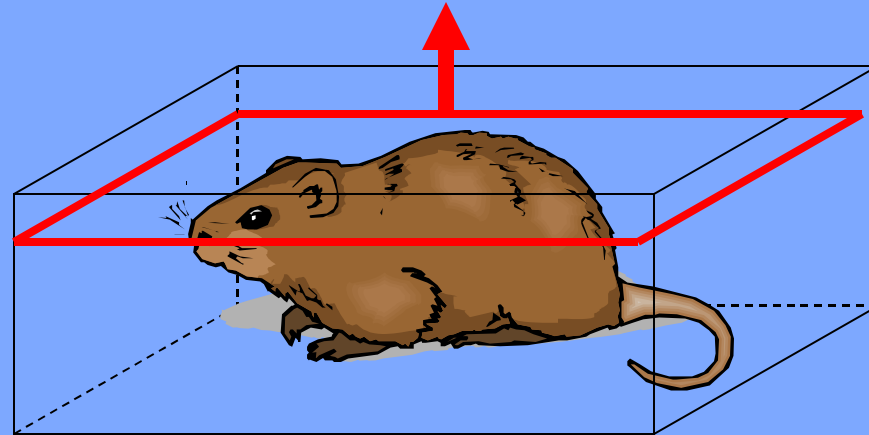




In Vivo Experiments

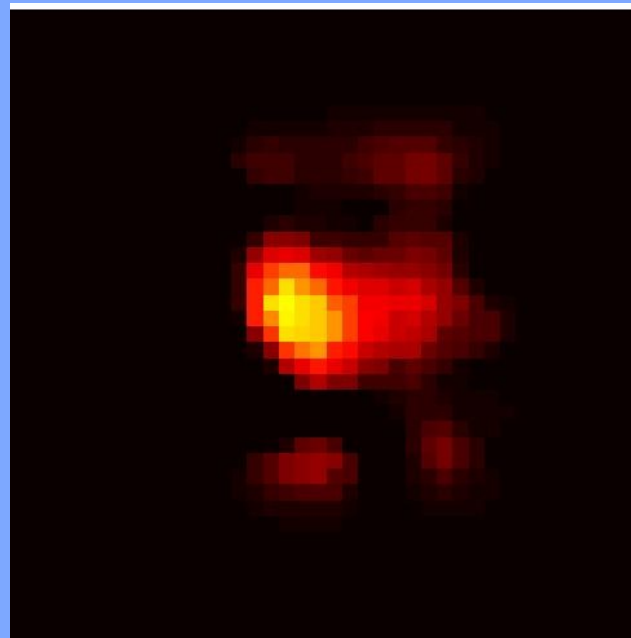
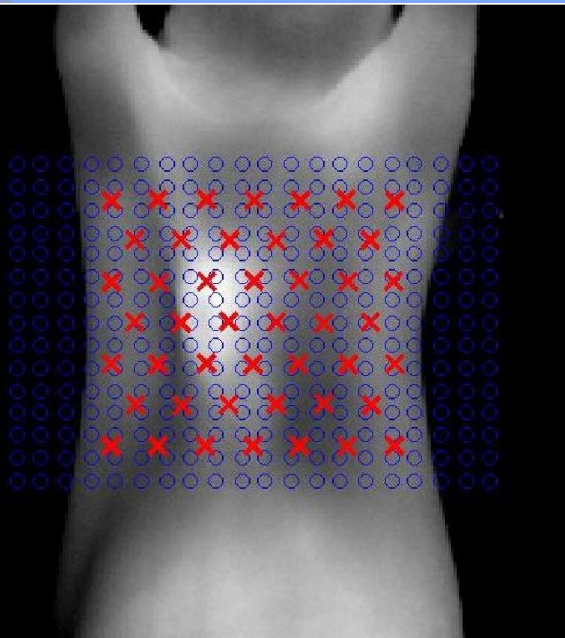
depth

0.2 cm



top view

fluorophore
absorption = 0 - 0.032 cm⁻¹

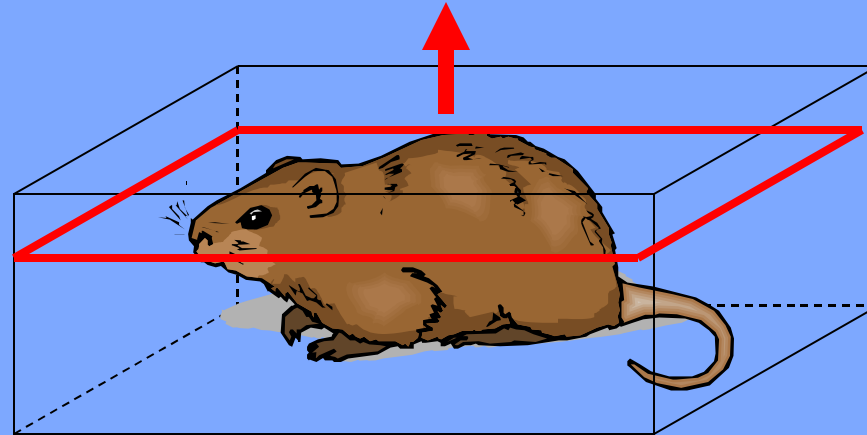




In Vivo Experiments

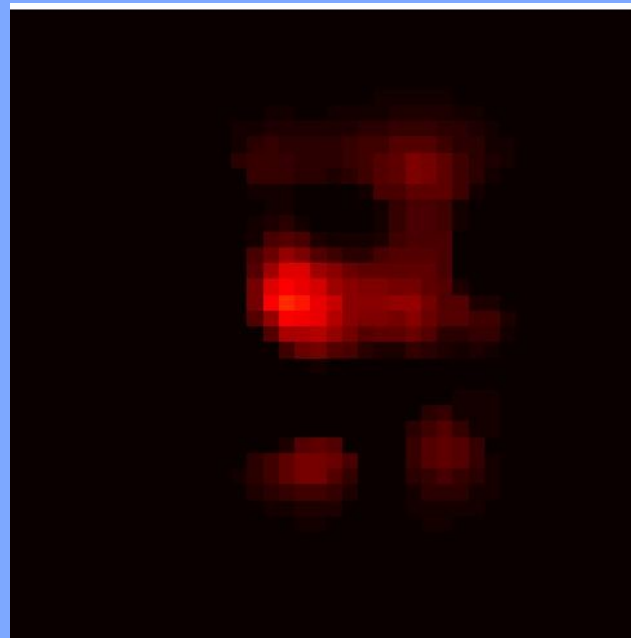
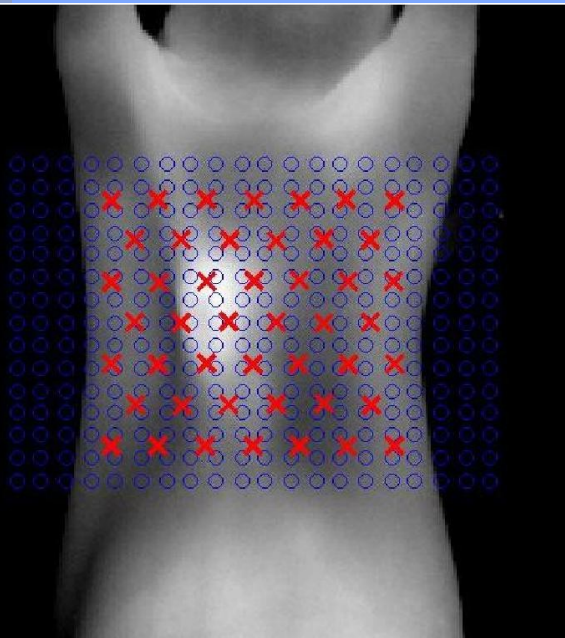
depth

0.3 cm



top view

fluorophore
absorption = 0 - 0.032 cm⁻¹

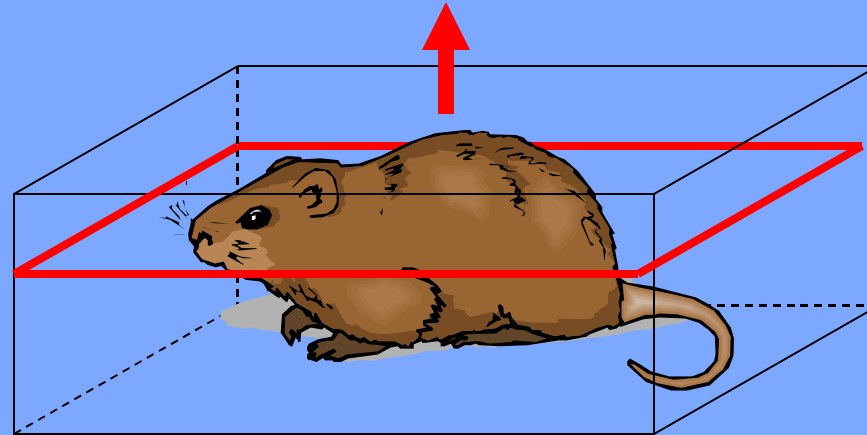




In Vivo Experiments

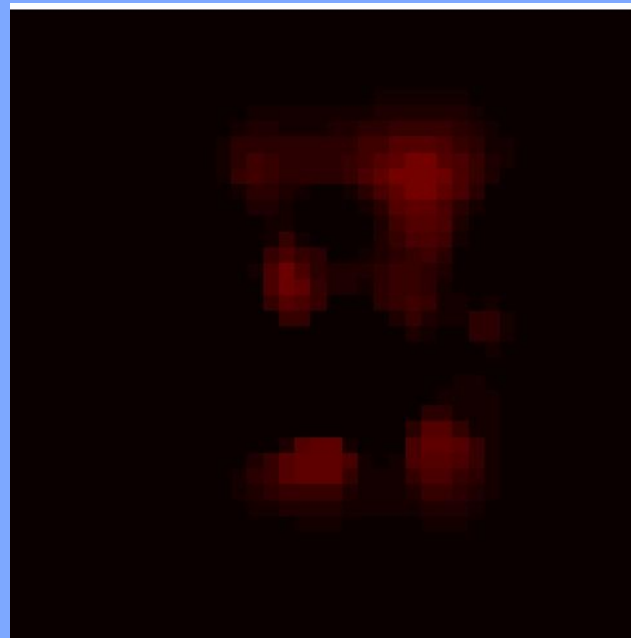
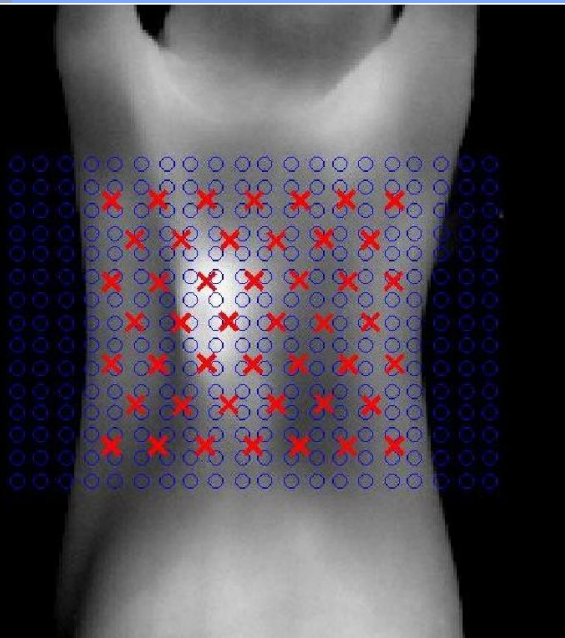
depth

0.4 cm



top view

fluorophore
absorption = 0 - 0.032 cm⁻¹

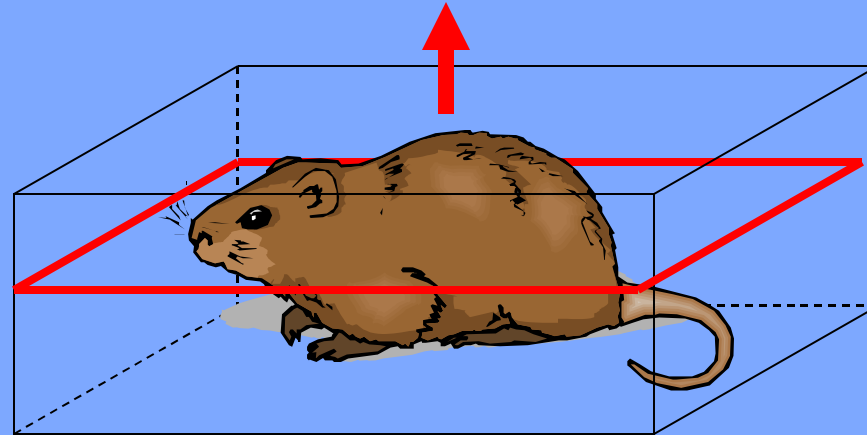




In Vivo Experiments

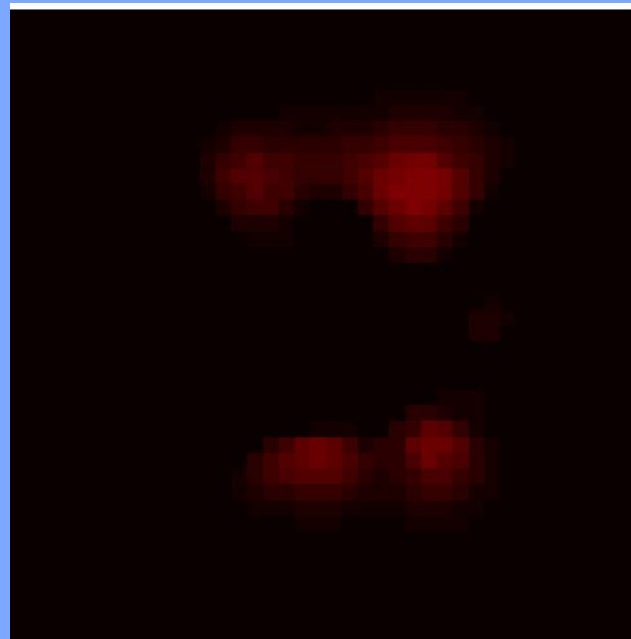
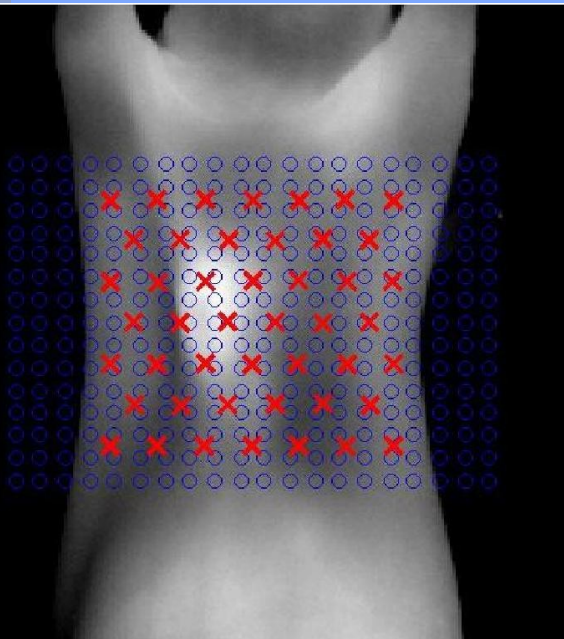
depth

0.5 cm



top view

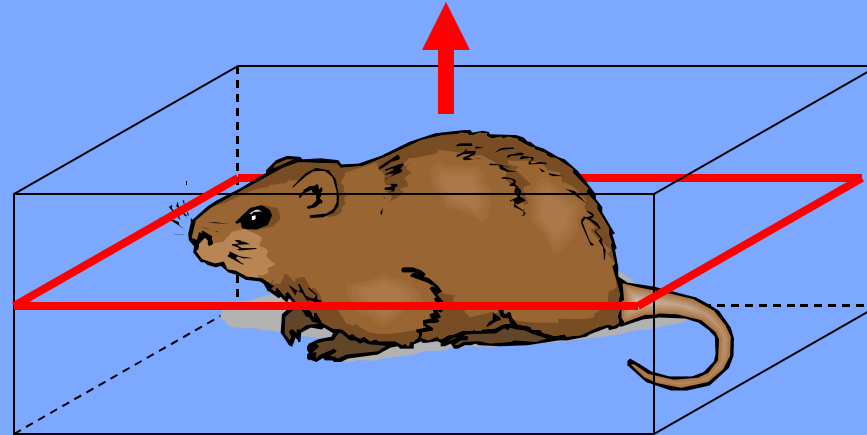
fluorophore
absorption = 0 - 0.032 cm⁻¹



In Vivo Experiments

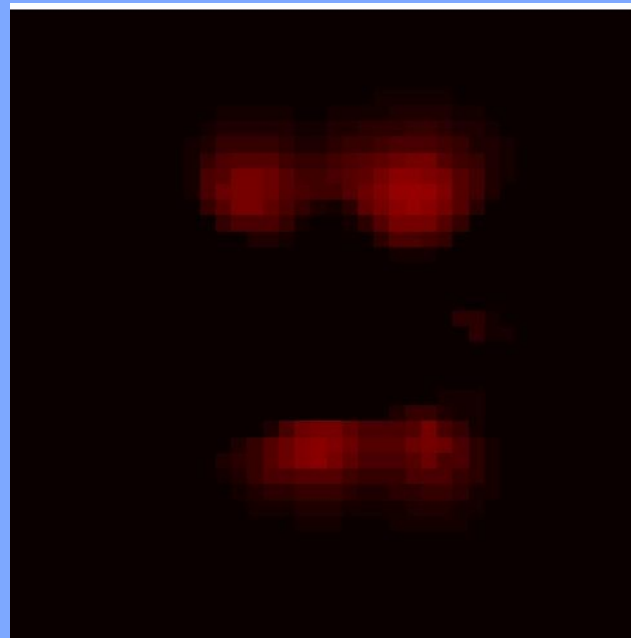
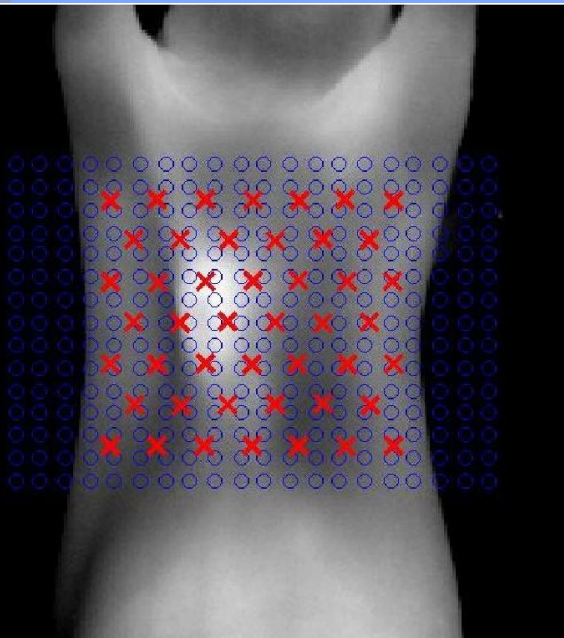
depth

0.6 cm



top view

fluorophore
absorption = 0 - 0.032 cm⁻¹

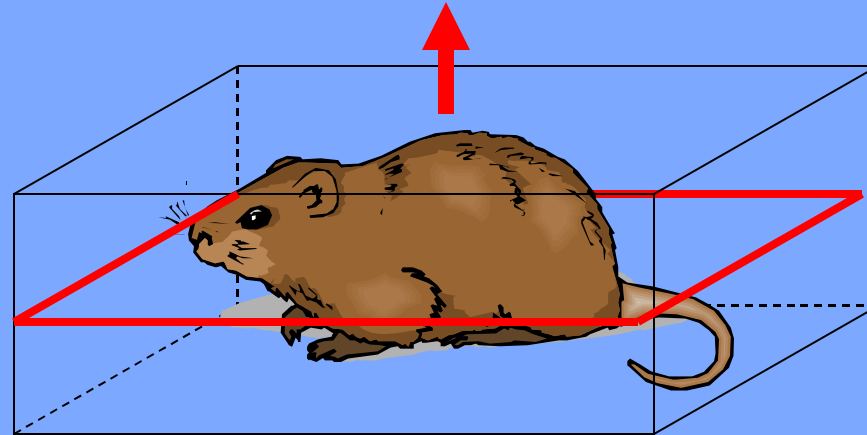




In Vivo Experiments

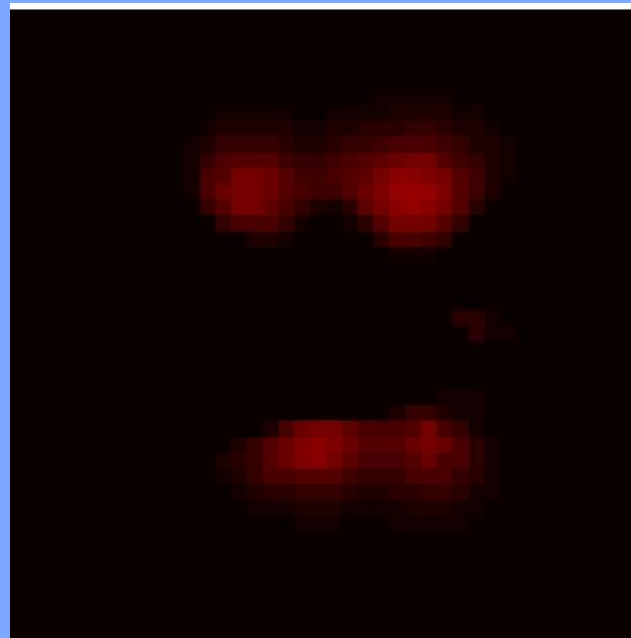
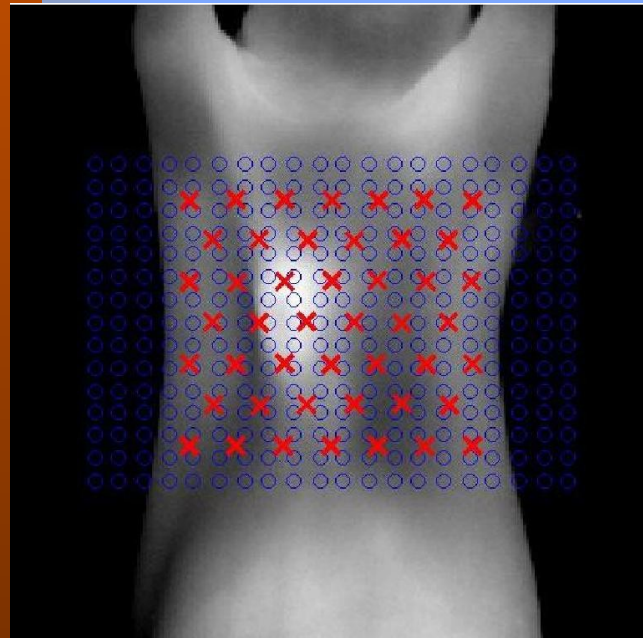
depth

0.7 cm



top view

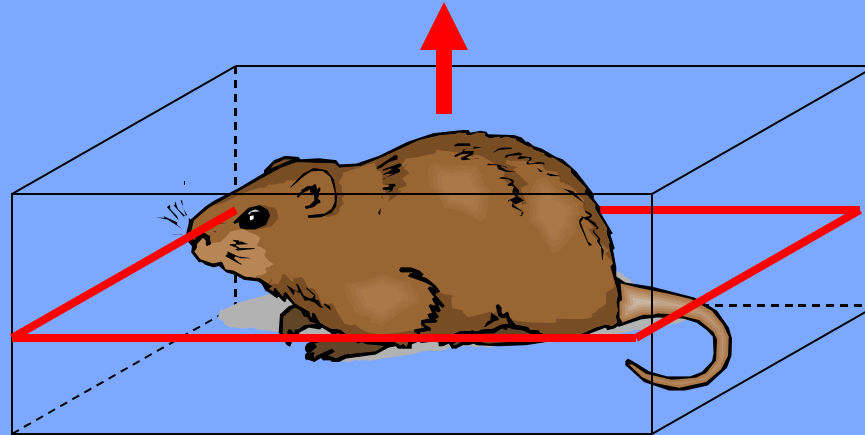
fluorophore
absorption = 0 - 0.032 cm⁻¹



In Vivo Experiments

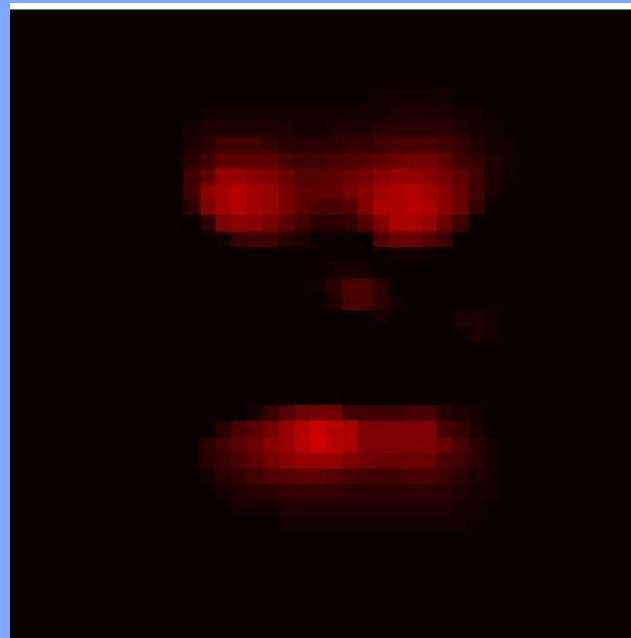
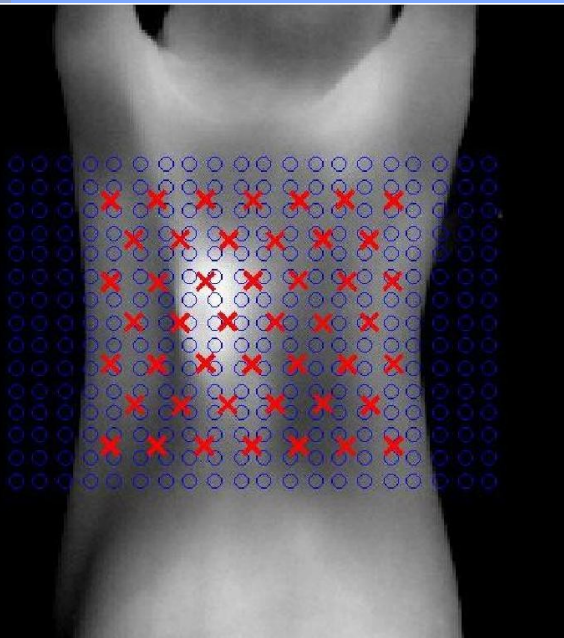
depth

0.8 cm



top view

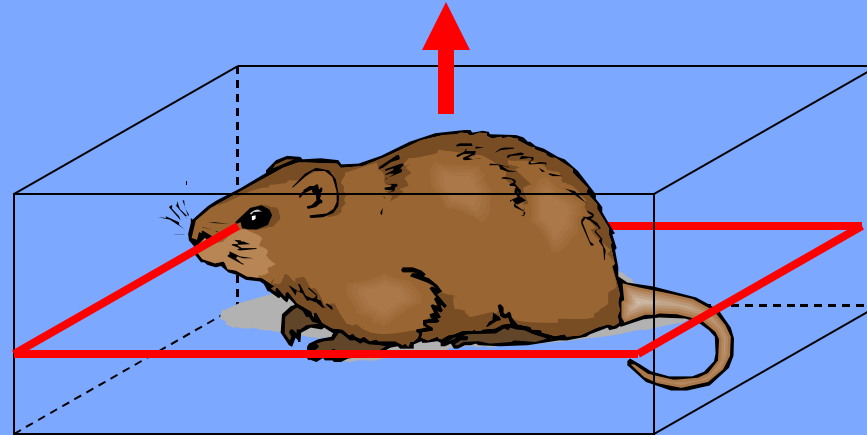
fluorophore
absorption = 0 - 0.032 cm⁻¹



In Vivo Experiments

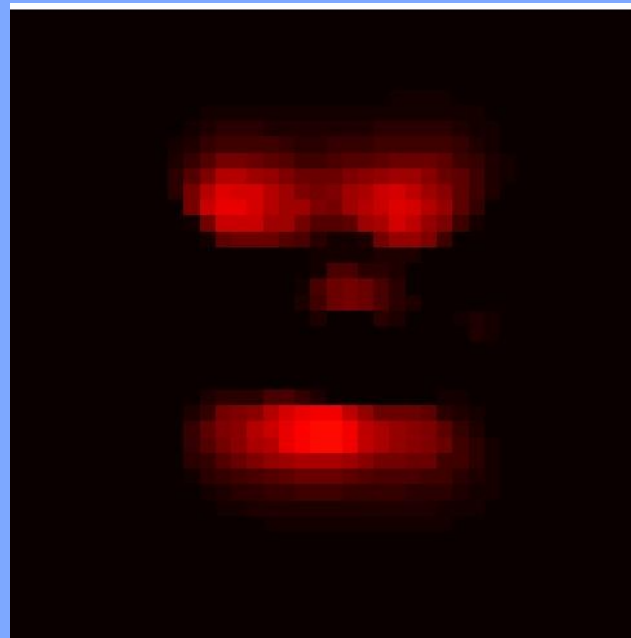
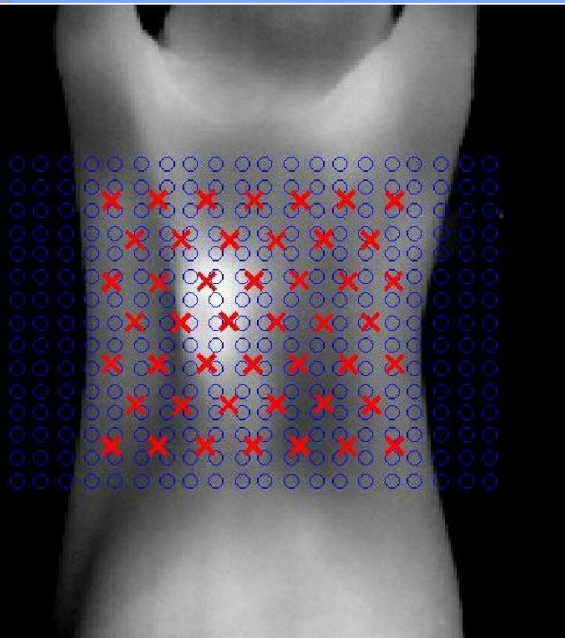
depth

0.9 cm



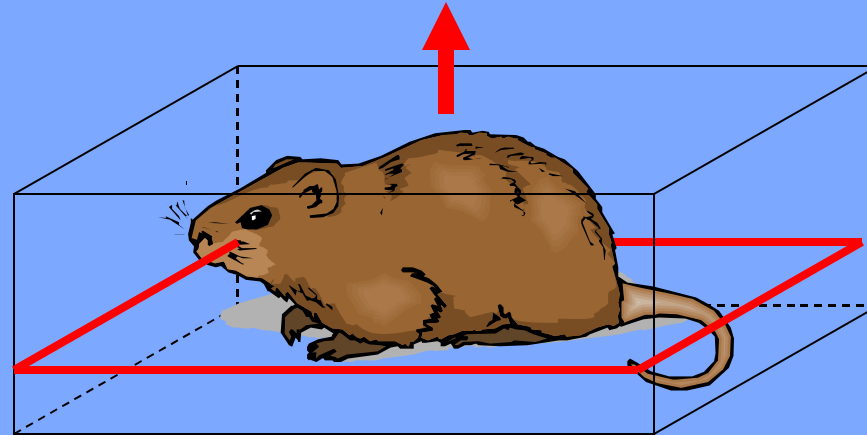
top view

fluorophore
absorption = 0 - 0.032 cm⁻¹



In Vivo Experiments

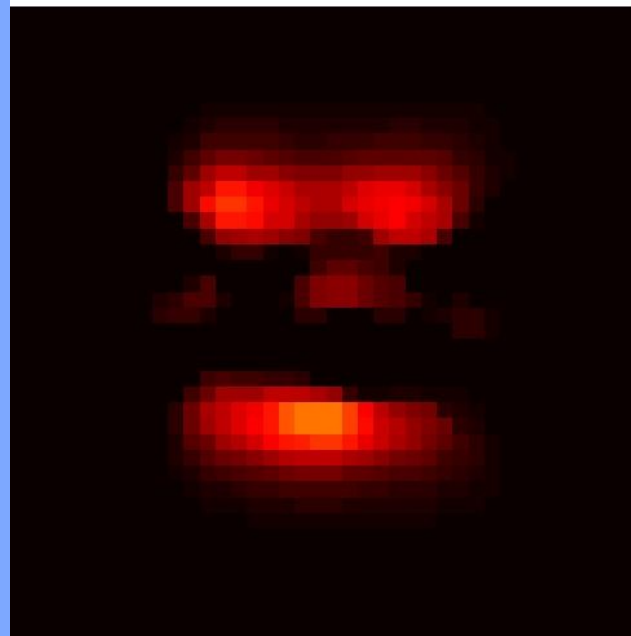
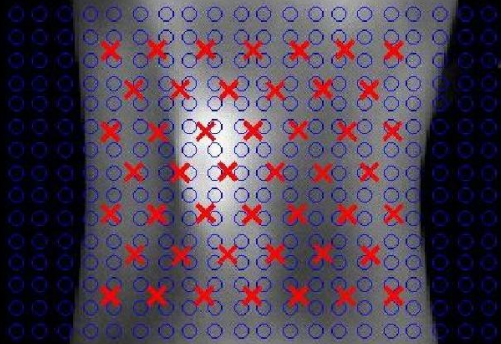
depth



1.0 cm

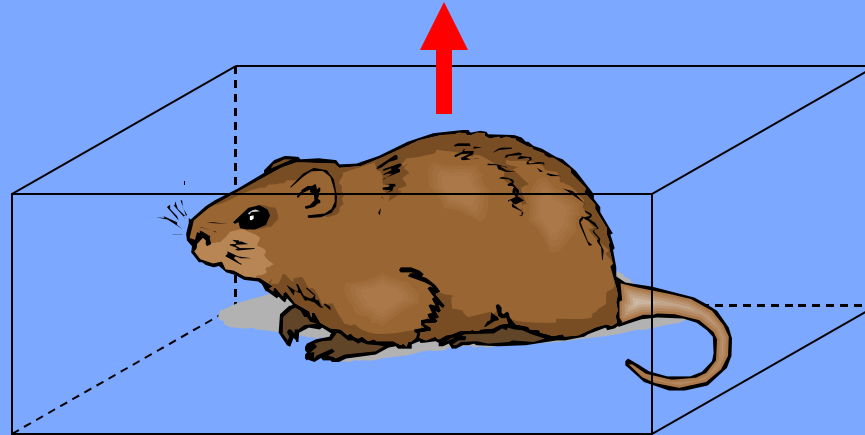
top view

fluorophore
absorption = 0 - 0.032 cm⁻¹



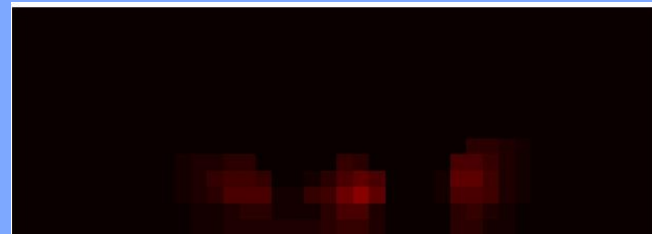
In Vivo Experiments

top view



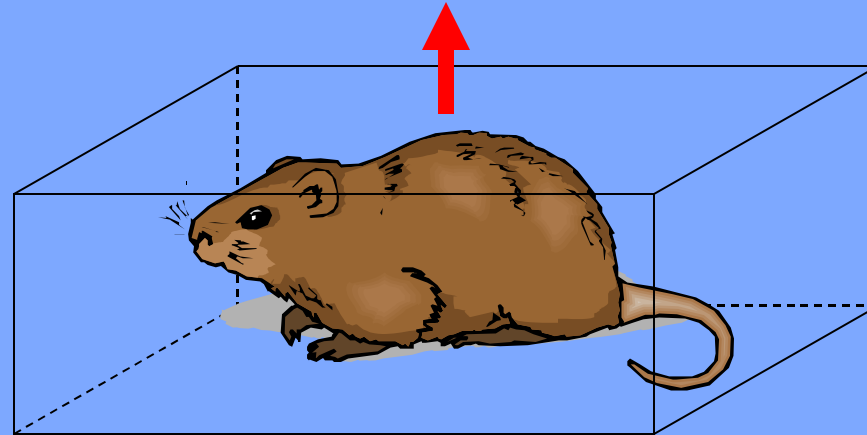
fluorophore
absorption = 0 - 0.032 cm⁻¹

+1.0 cm



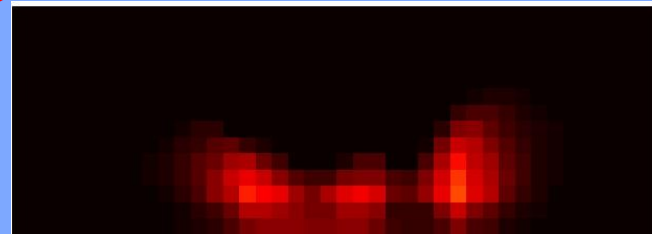
In Vivo Experiments

top view



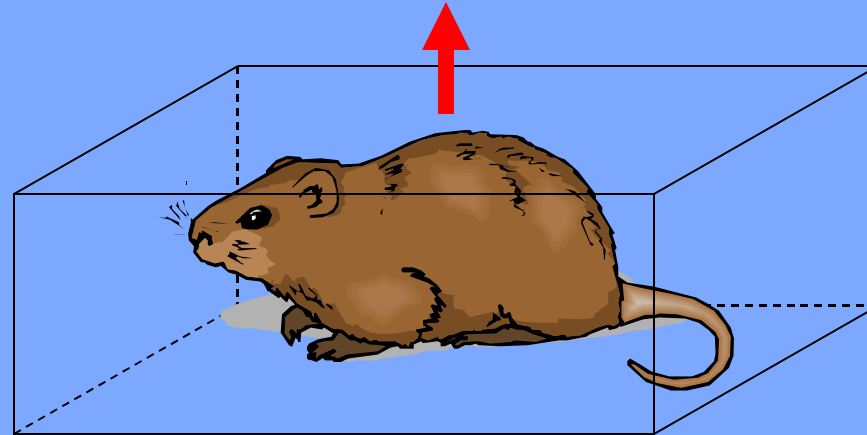
fluorophore
absorption = 0 - 0.032 cm⁻¹

+0.8 cm



In Vivo Experiments

top view



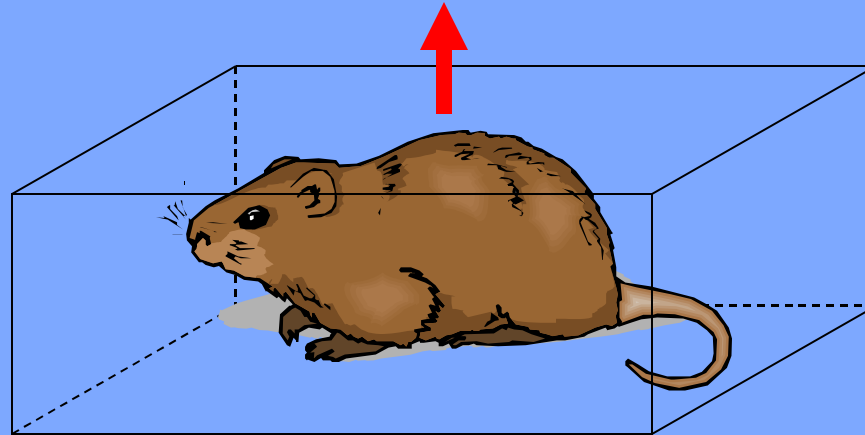
fluorophore
absorption = 0 - 0.032 cm⁻¹

+0.6 cm

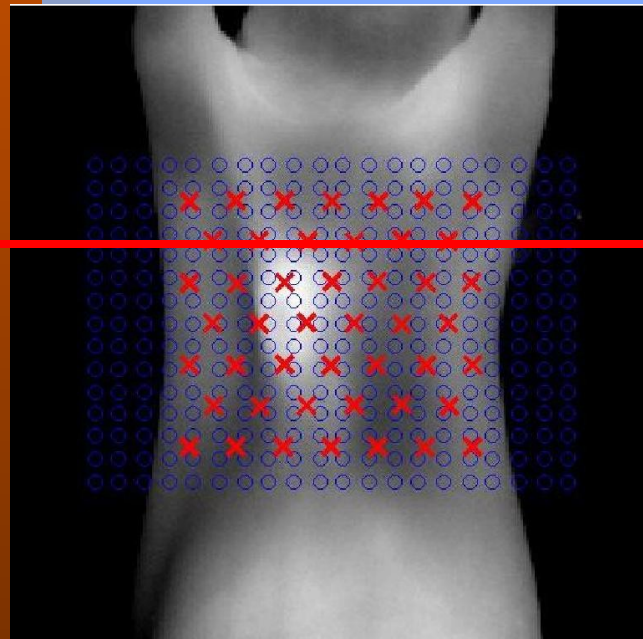


In Vivo Experiments

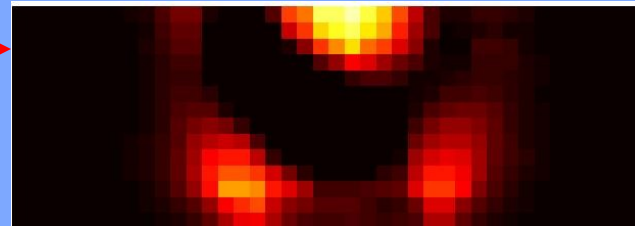
top view



fluorophore
absorption = 0 - 0.032 cm⁻¹

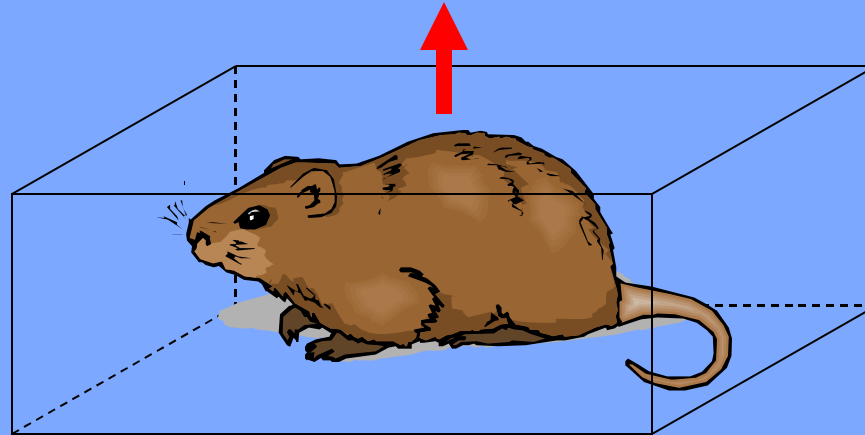


+0.4 cm

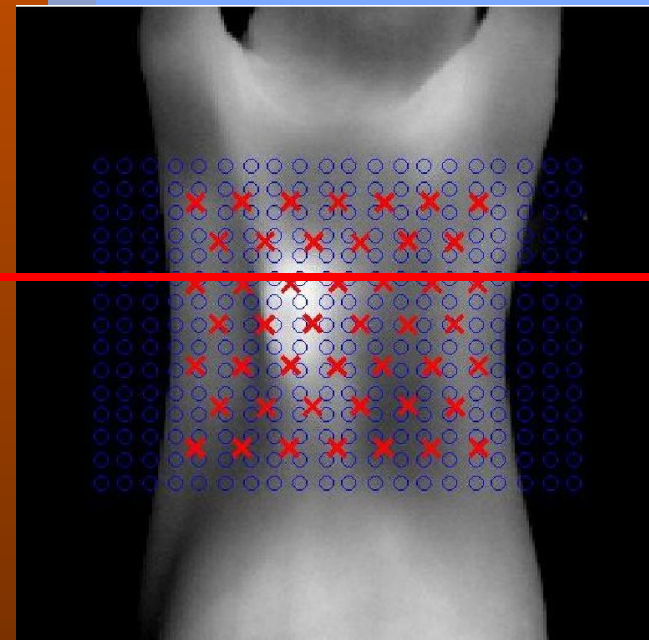


In Vivo Experiments

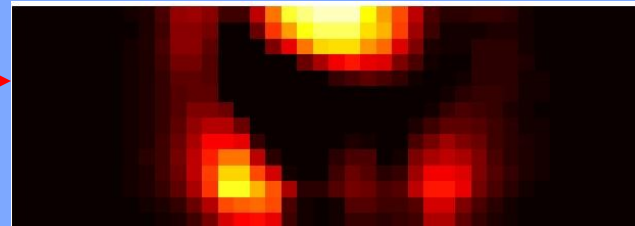
top view



fluorophore
absorption = 0 - 0.032 cm⁻¹

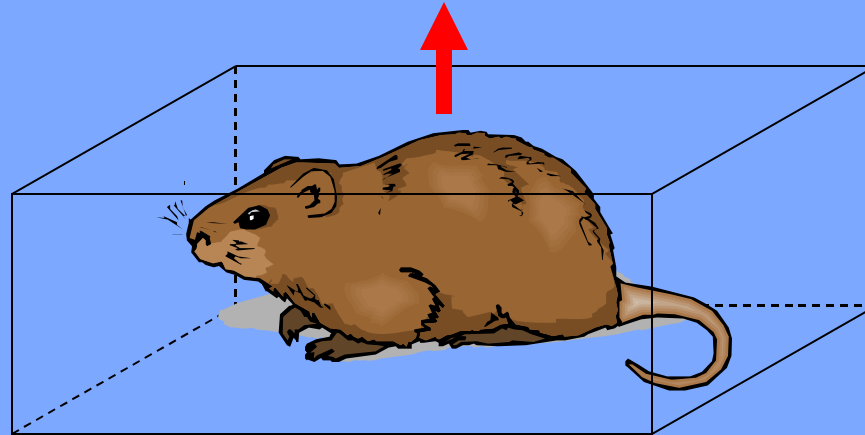


+0.2 cm

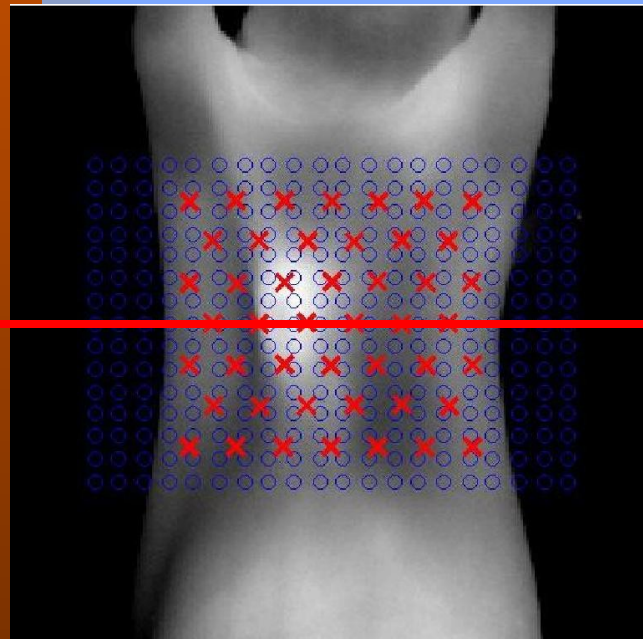


In Vivo Experiments

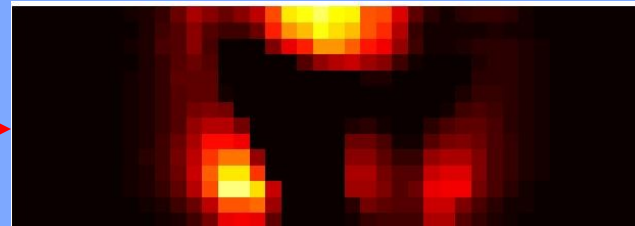
top view



fluorophore
absorption = 0 - 0.032 cm⁻¹

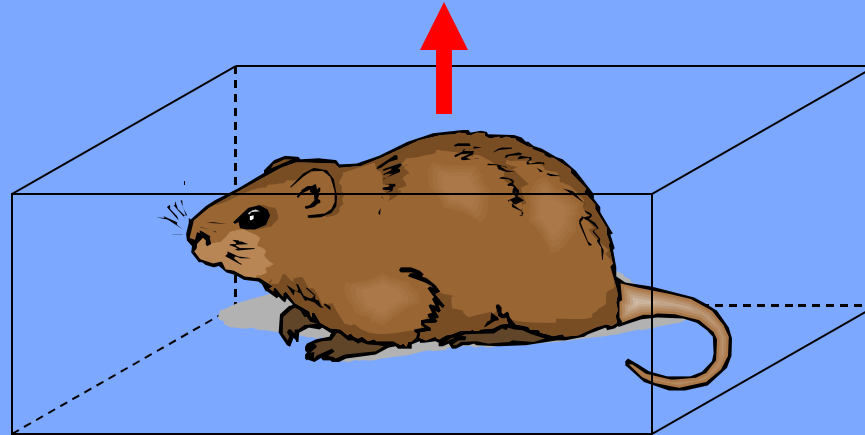


0 cm

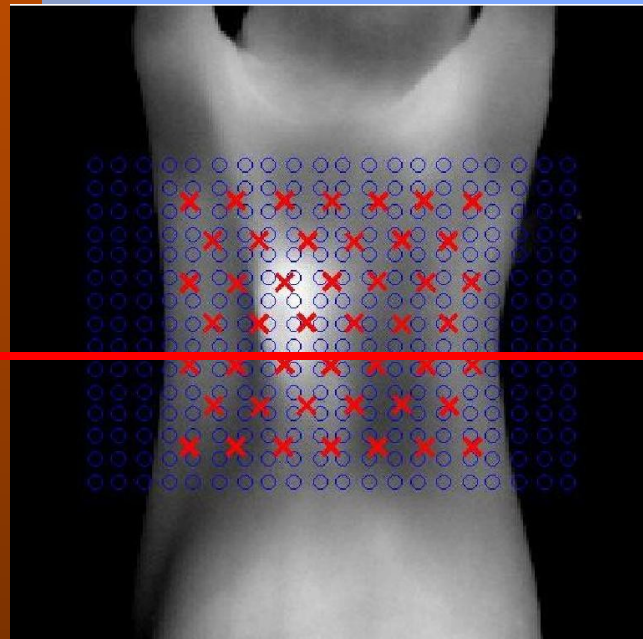


In Vivo Experiments

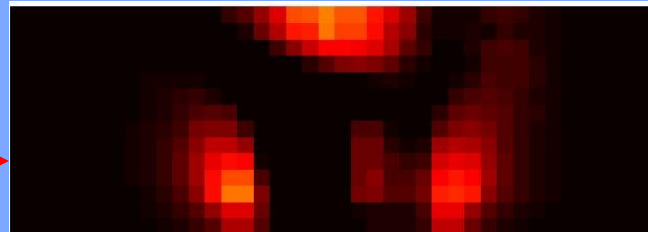
top view



fluorophore
absorption = 0 - 0.032 cm⁻¹

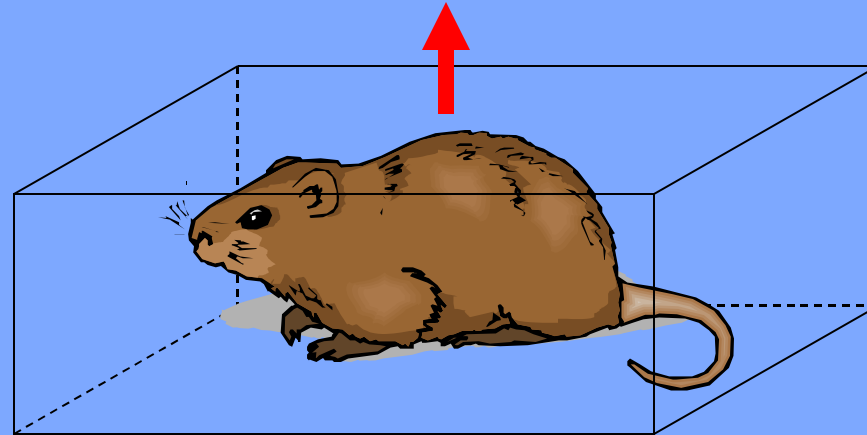


-0.2 cm

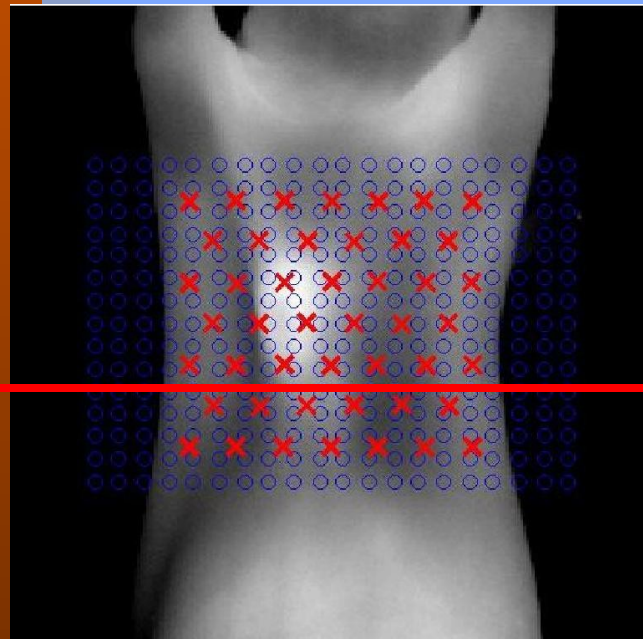


In Vivo Experiments

top view



fluorophore
absorption = 0 - 0.032 cm⁻¹

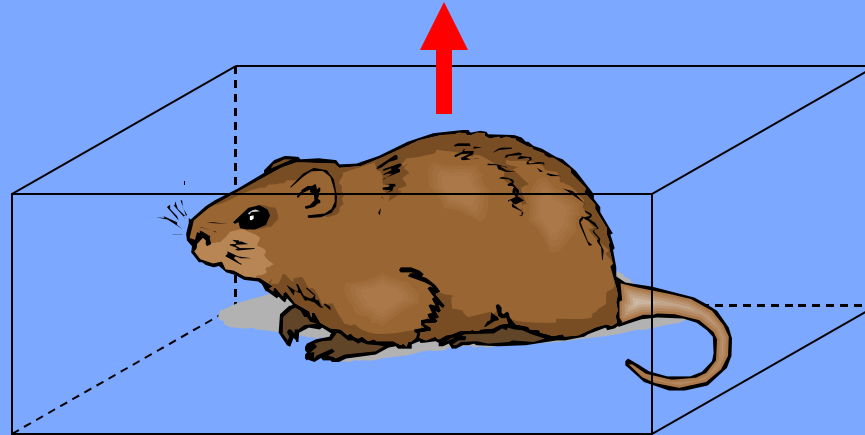


-0.4 cm

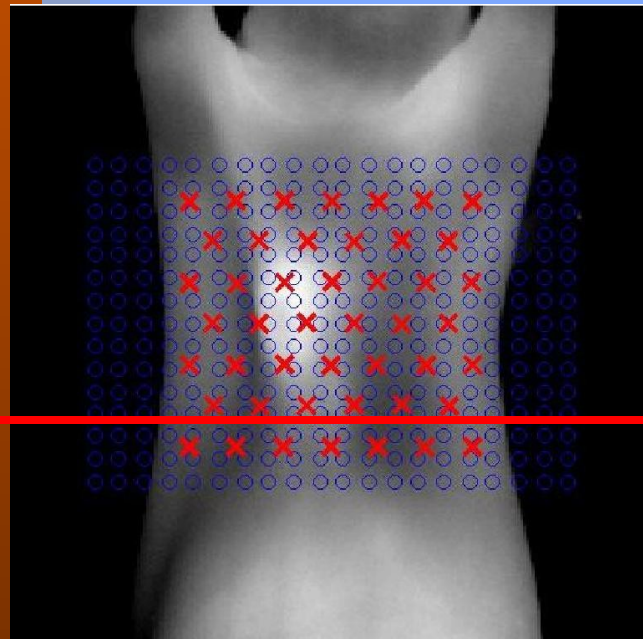


In Vivo Experiments

top view



fluorophore
absorption = 0 - 0.032 cm⁻¹

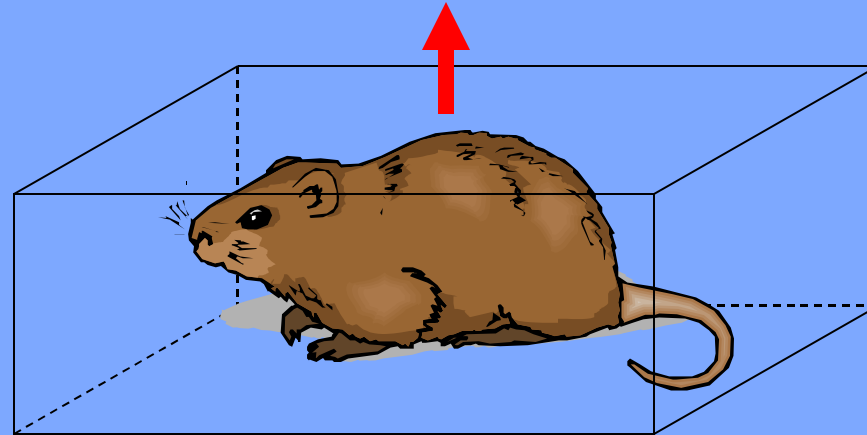


-0.6 cm

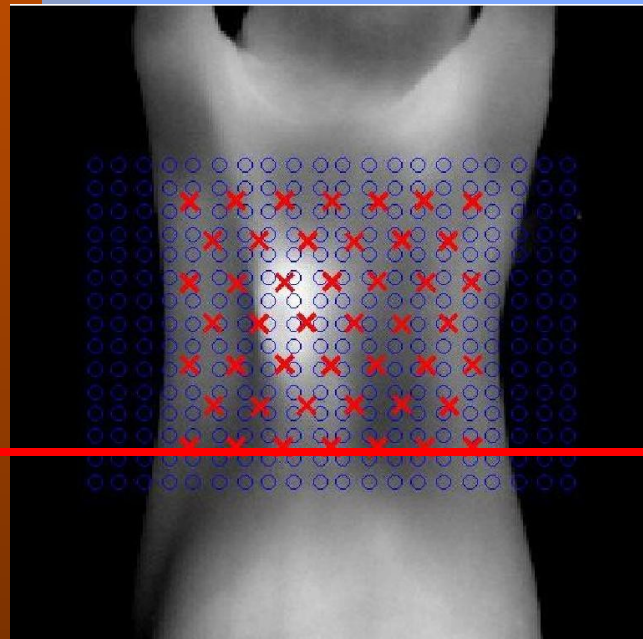


In Vivo Experiments

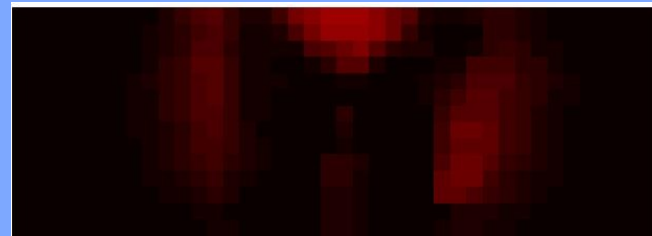
top view



fluorophore
absorption = 0 - 0.032 cm⁻¹

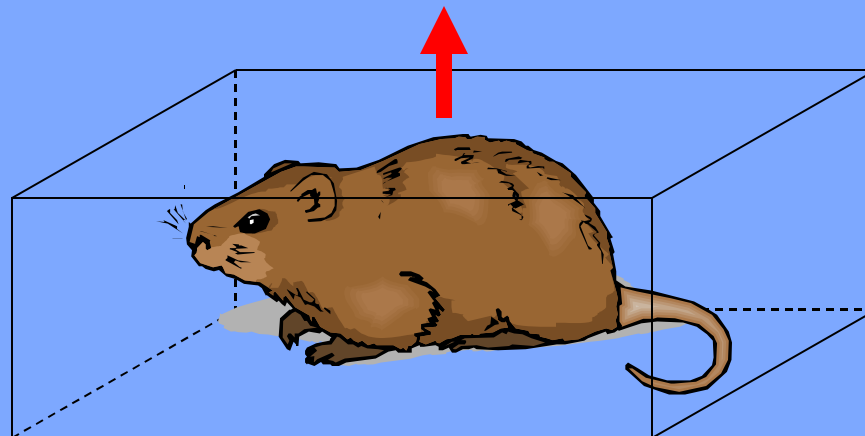


-0.8 cm

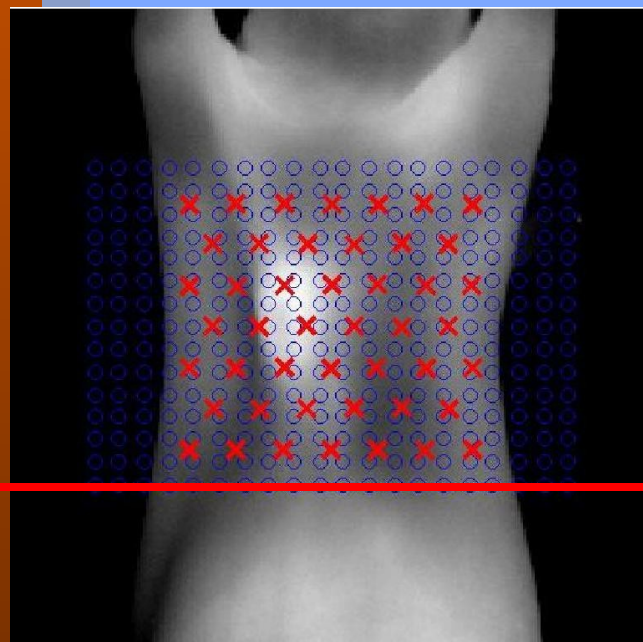


In Vivo Experiments

top view



fluorophore
absorption = $0 - 0.032 \text{ cm}^{-1}$





Overview

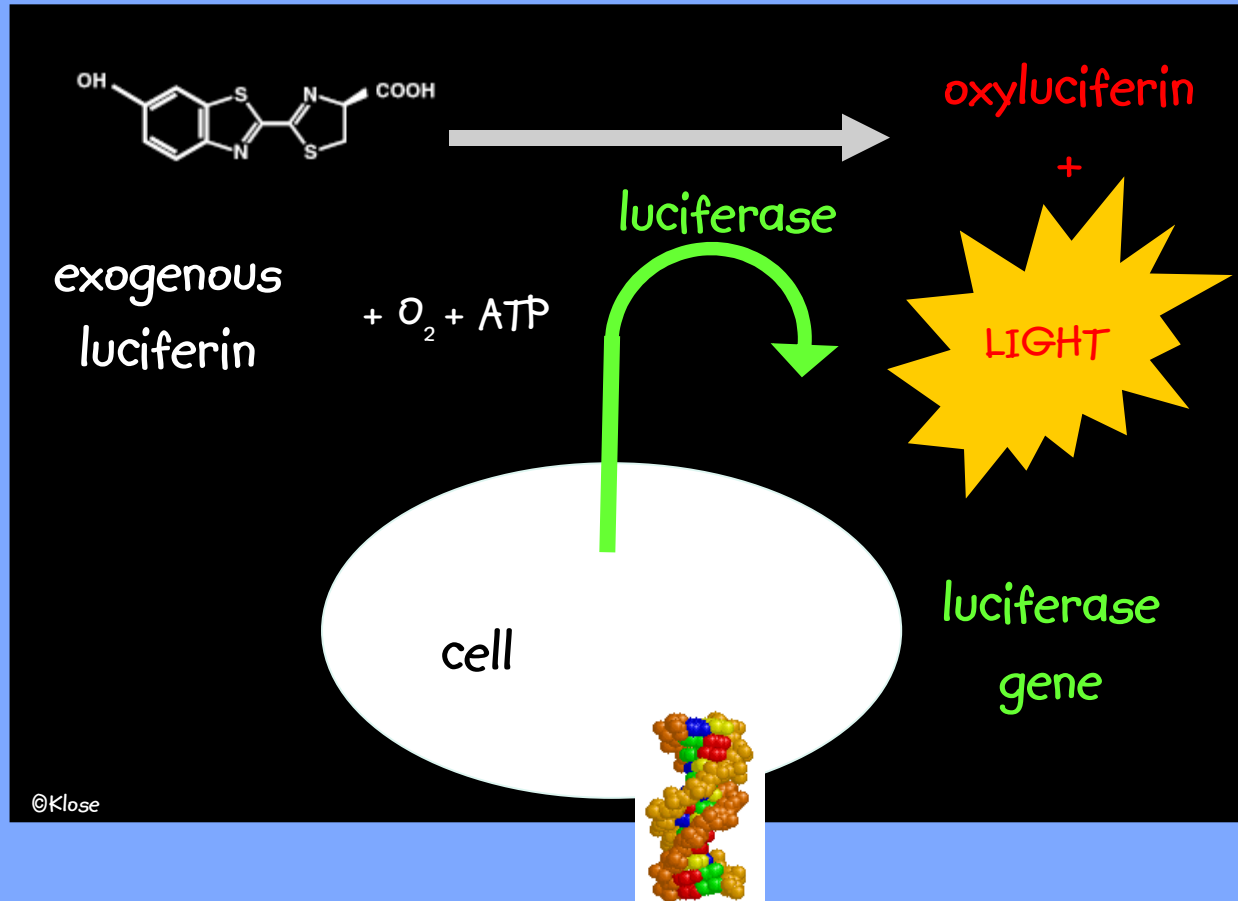
Forward Model

Inverse Model

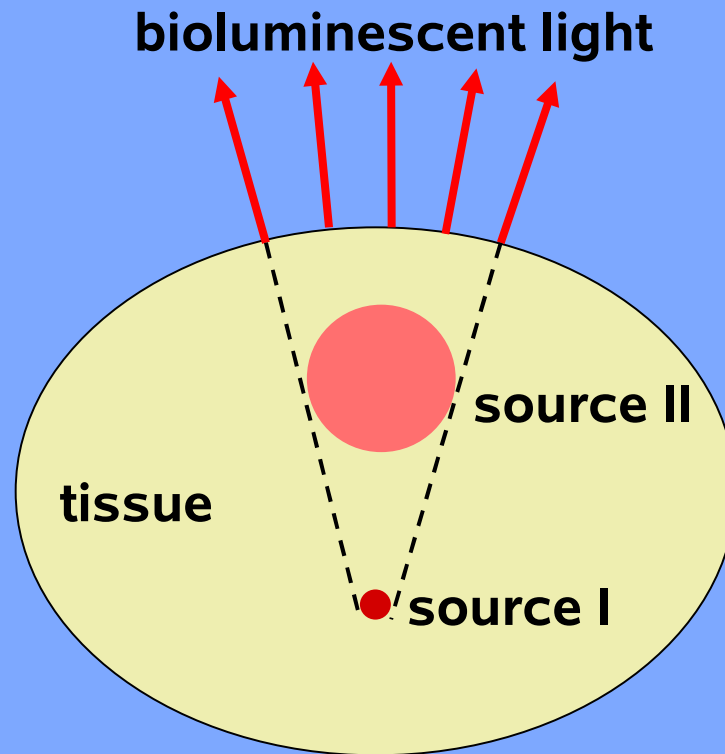
Fluorescence Molecular Tomography

Bioluminescence Tomography

Bioluminescence Tomography



Multiple Solutions

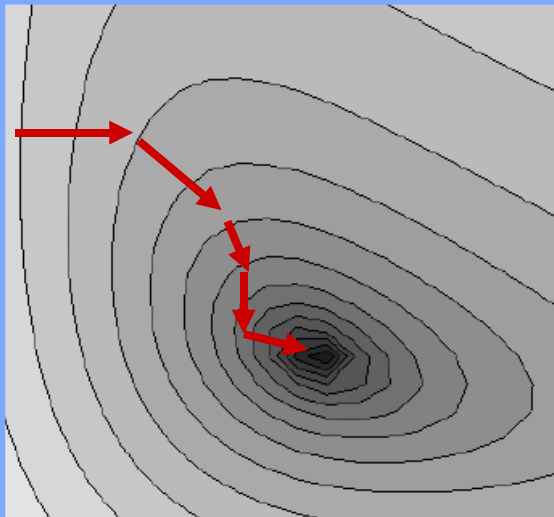


$$\phi(\theta) = \frac{1}{N} \sum_n \frac{(Y_n - J_n^+(\theta))^2}{\sigma_n^2}$$

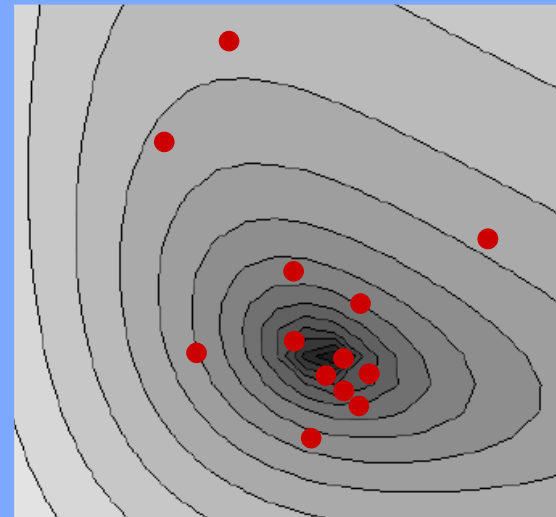
Optimization of

$$\phi(\theta) = \frac{1}{N} \sum_n \frac{(Y_n - J_n^+(\theta))^2}{\sigma_n^2}$$

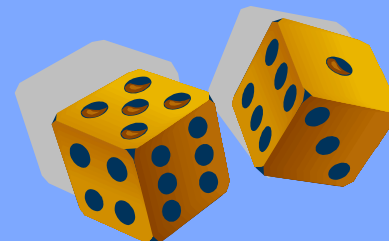
deterministic



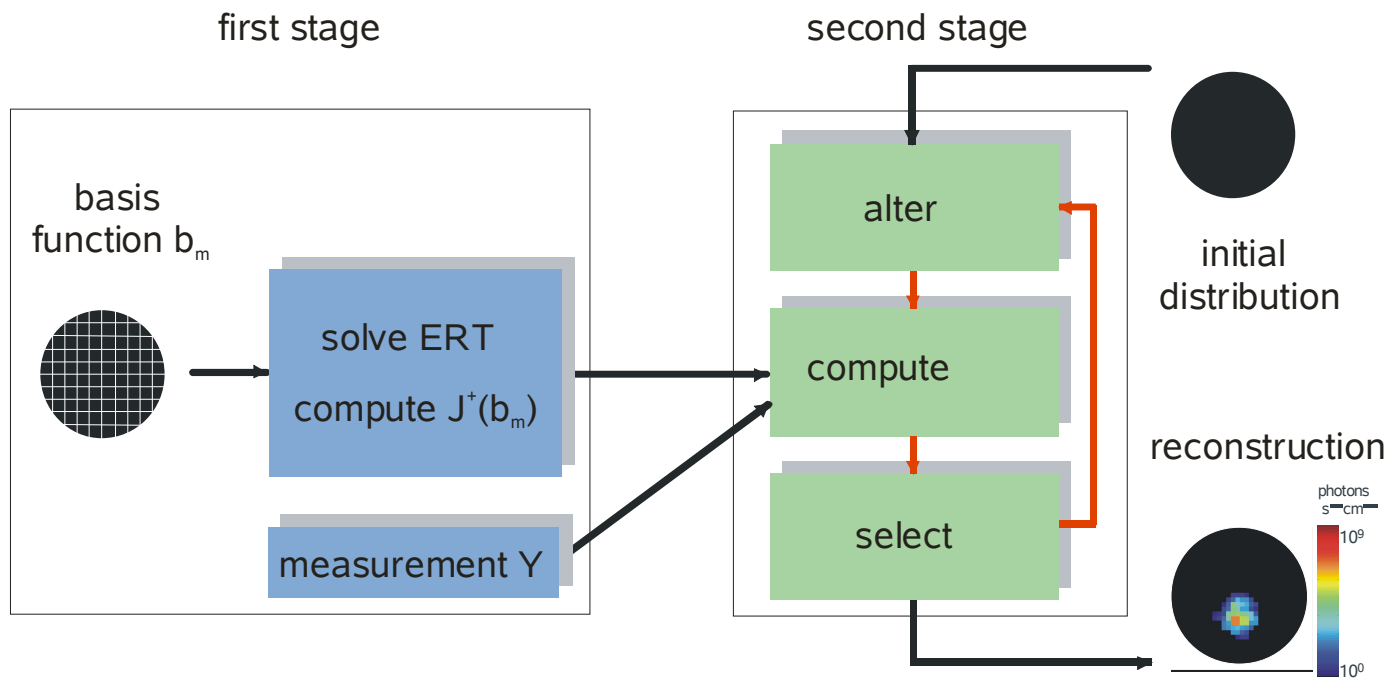
stochastic



$$\nabla \phi = \frac{(J^+ - Y)}{2\sigma^2} \frac{\partial J^+}{\partial Q}$$



Stochastic Image Reconstruction (SIR)





First Stage - Linear Source problem

source power density is decomposed
into source basis functions b_m

$$Q(r) = \sum_{m=0}^M \theta_m b_m(r)$$

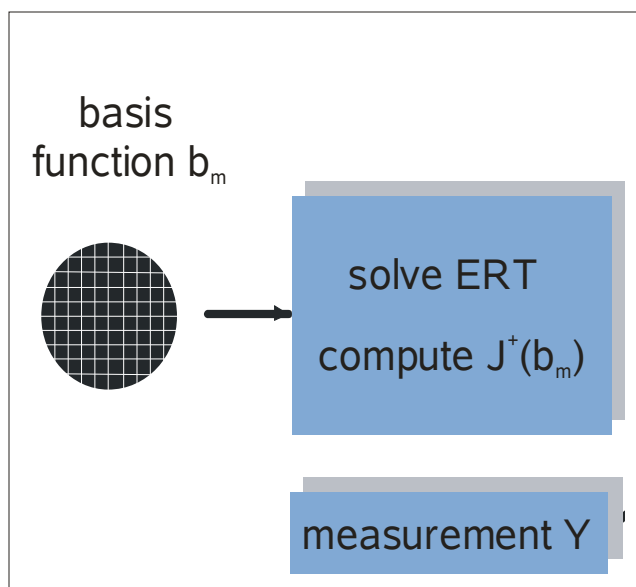
$$\Omega \cdot \nabla \psi(r, \Omega) + \mu_t \psi(r, \Omega) = \frac{b_m(r)}{4\pi} + \mu_s \int_{4\pi} p(\Omega, \Omega') \psi(r, \Omega') d\Omega'$$

boundary flux as function of unknown
data variables θ_m

$$J_n(\theta) = \sum_{m=0}^M \theta_m J_n(b_m)$$

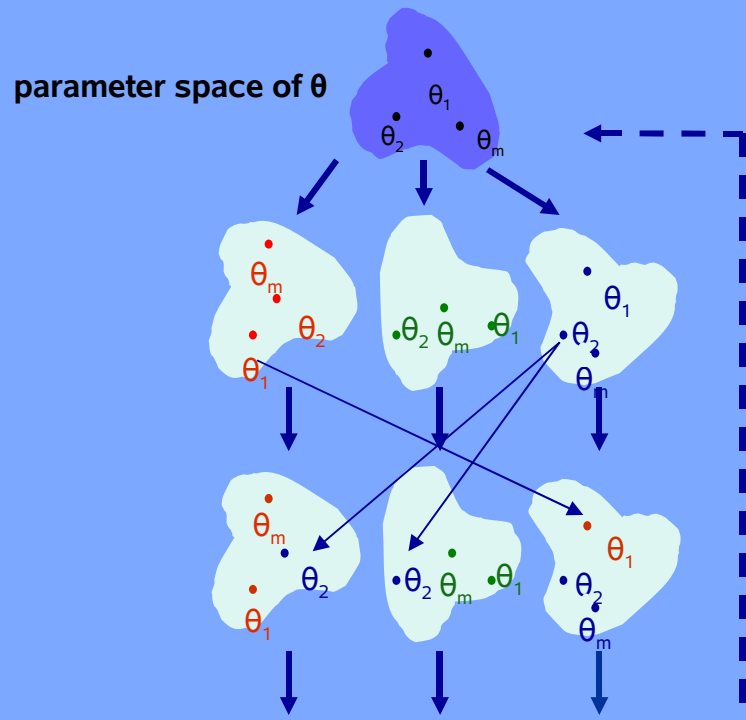
Stochastic Image Reconstruction (SIR)

first stage



Second Stage - Evolution Strategy

1. Alter θ :



population of μ parents

population of λ offspring

recombination
self-adaptation
mutation

$$\theta_m^{\text{new}} = \theta_m^{\text{old}} + N(0, \sigma_m)$$

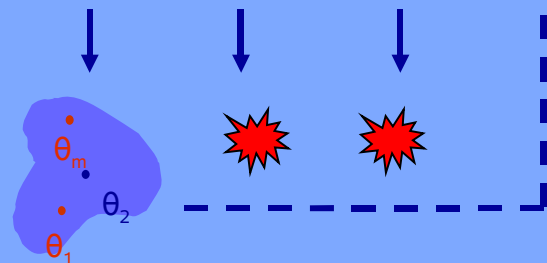
2. Compute Φ :

$$\Phi(\theta) = \frac{1}{N} \sum_n \frac{(Y_n - J_n^+(\theta))^2}{\sigma_n^2}$$

select smallest Φ

“survival of the fittest”

3. Select θ :



NEW
population of μ parents

Second Stage – Evolution Strategy

- **Recombination:**

$$\theta_m^\lambda = \frac{\theta_a^\mu + \theta_b^\mu}{2}$$

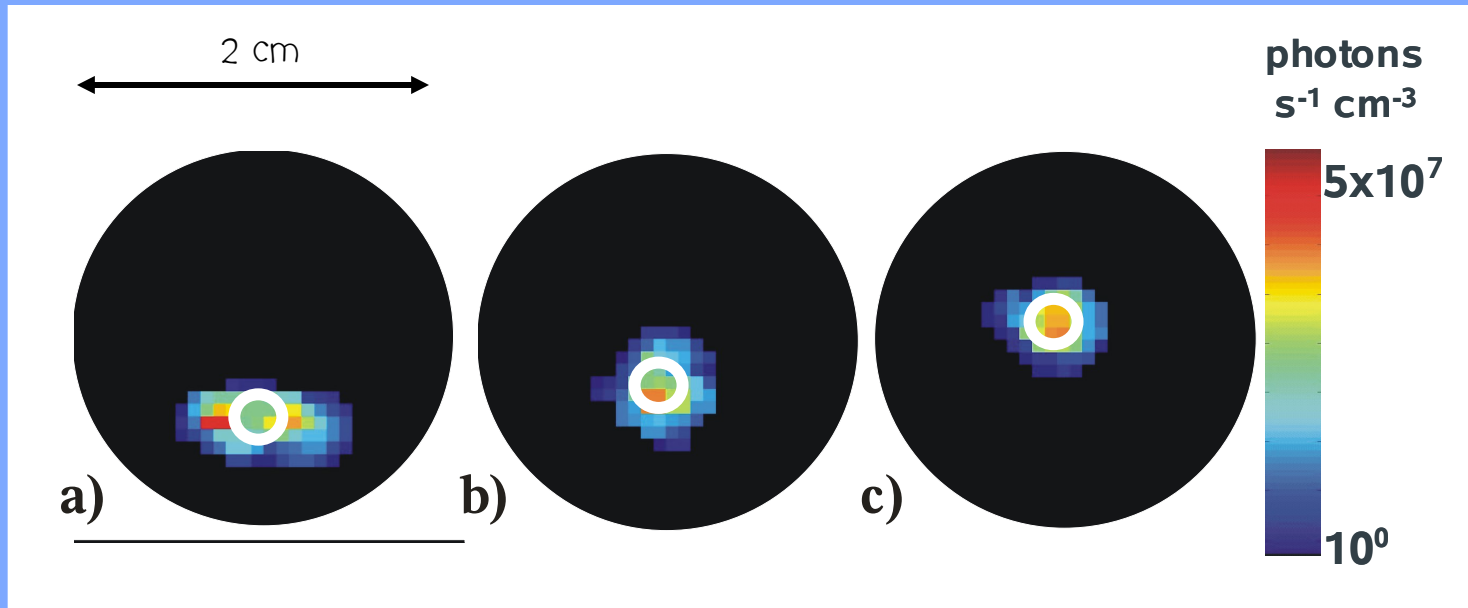
- **Self-Adaptation:**

$$\hat{\sigma}_m^\lambda = \sigma_m^\lambda e^{\tau N(0,1)}$$

- **Mutation:**

$$\hat{\theta}_m^\lambda = \theta_m^\lambda + N(0, \hat{\sigma}_m^\lambda)$$

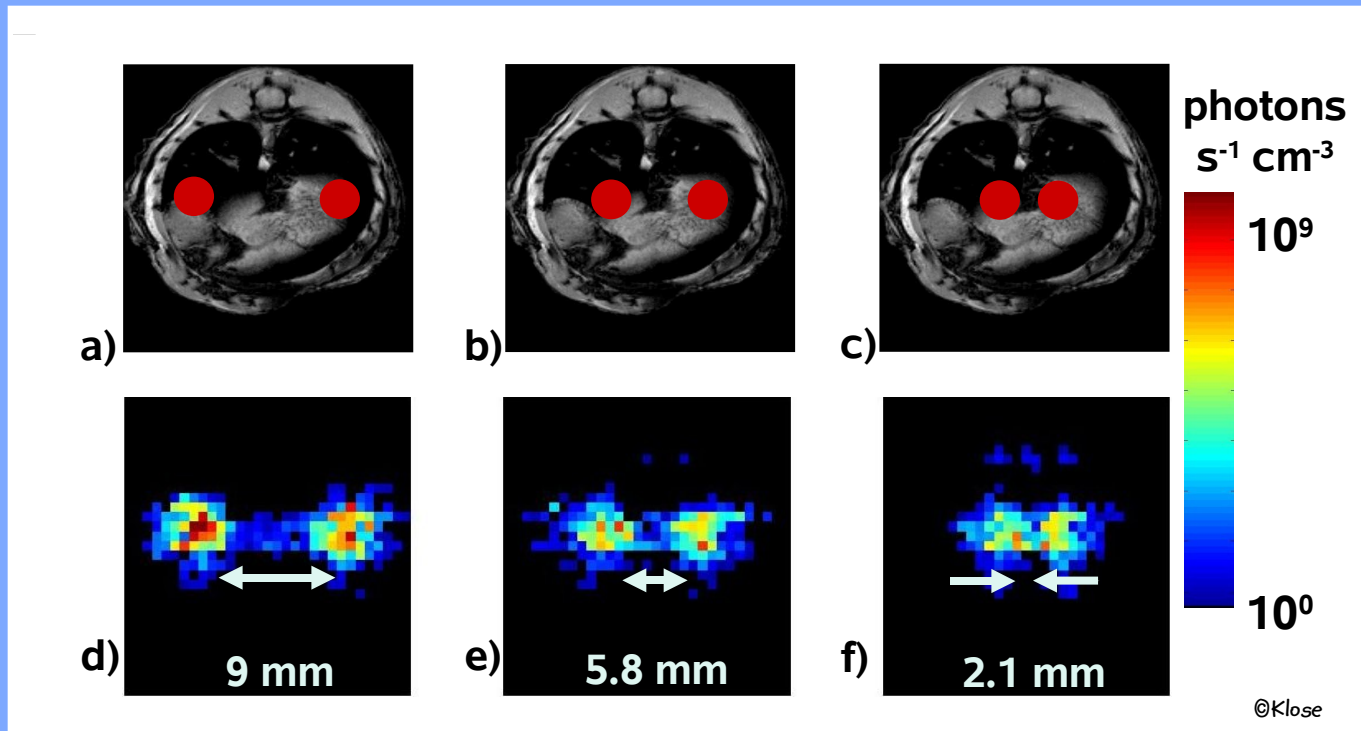
Results - Simulations



675 unknown vector elements θ_m (image)

$\mu = 3,000$ parent members; $\lambda = 18,000$ offspring members
900 generations

Results - Simulations



Tomographic reconstruction of two bioluminescent sources.
Optical property maps are based on MRIs.



Summary

Optical Molecular Imaging

- fluorescent/bioluminescent probes

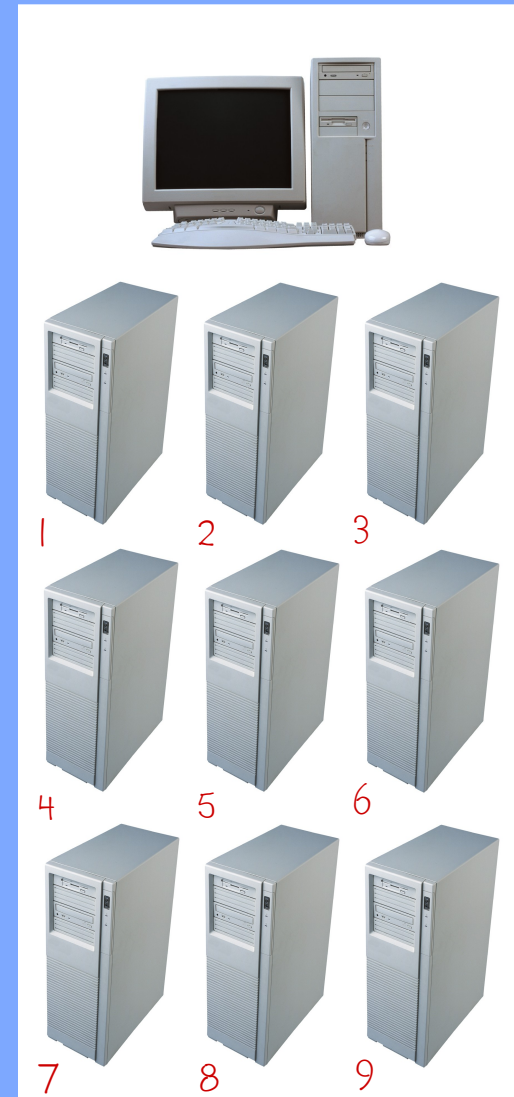
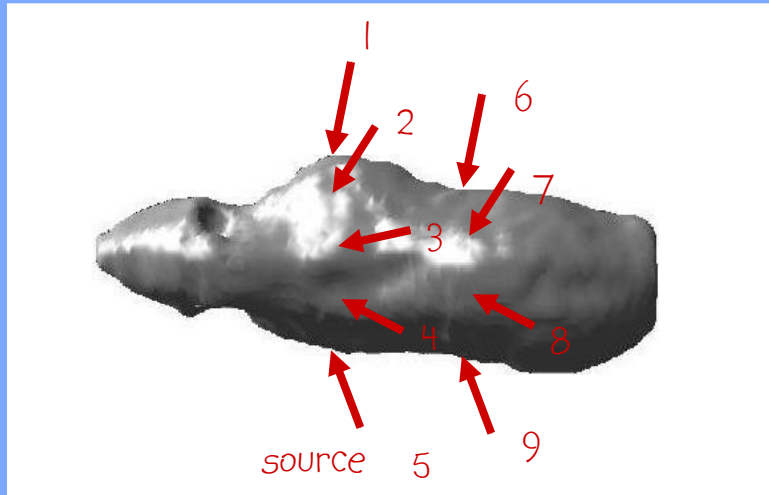
Biological tissue is highly scattering

- Equation of Radiative Transfer
- Finite-Difference Discrete-Ordinates (FD- S_N)

Inverse source problem

- optimization methods
 - gradient techniques (Adjoint Differentiation)
 - Evolution Strategy

Future Work



Field Programming Gate Array (FPGA) ?



Acknowledgments

- Edward Larsen (University of Michigan)
- Ken Hanson (Los Alamos National Lab)
- Vasilis Ntziachristos (Harvard Medical School)

www.columbia.edu/~ak2083/publications.htm